SWOT-Nadir validation and cross calibration activities

Executive Summary - Annual Report 2024

Reference: SALP-RP-MA-EA-23679-CLS

Issue: 1.3

Date: December 31, 2025

Contract: SALP 2023-24 No 221332

Customer:	CNES	**Document Ref.:**	SALP-RP-MA-EA-23679-CLS
Contract :	SALP 2023-24 No 221332	**Date:**	December 31, 2025
		Issue	1.3

Project:	MISSION PERFORMANCE SERVICE FOR SN MISSION		
Title:	SWOT-Nadir validation and cross calibration activities Annual Report 2024		
	Name	**Company**	**Date**
Author(s):	N. Kientz A. Deniau & H. Roinard T. Pirotte	ALTEN for CLS CLS CLS	
Approved by:	F. Bignalet-Cazalet	CNES	
Application authorized by :			

Change Log

Version	Date	Changes
1.0	March 31, 2025	Creation
1.1	May 12, 2025	Several improvements
1.2	May 27, 2025	Executive report
1.3	December 31, 2025	Missing data information Corrected

Acronyms

AMR Advanced Microwave Radiometer

CLS Collecte Localisation Satellites

CMEMS Copernicus Marine Service

CNES Centre National d'Etudes Spatiales

CNG Consigne Numerique de Gain (= Automatic Gain Control)

C2N Cryosat-2

DAC Dynamical Atmospheric Correction

DEM Digital Elevation Model

DV Default Value

DIODE Détermination Immédiate d'Orbite par Doris Embarqué

DORIS Doppler Orbitography and Radiopositioning Integrated by Satellite

DUACS Data Unification and Altimeter Combination System

ECMWF European Centre for Medium-range Weather Forecasting

FES Finite Element Solution

GDR Geophysical Data Record

GIM Global Ionosphere Maps

GMSL Global Mean Sea Level

GOT Global Ocean Tide

GPS Global Positioning System

IGDR Interim Geophysical Data Record

JPL Jet Propulsion Laboratory (Nasa)

L2P Along-track Sea Level Anomalies Level-2+

MLE Maximum Likelyhood Estimator

MOE Medium Orbit Ephemeris

MQE Mean Quadratic Error

MSS Mean Sea Surface

OGDR Operational Geophysical Data Record

PLTM PayLoad TeleMetry

POE Precise Orbit Ephemeris

POS-3C POSEIDON-3C

SALP Service d'Altimétrie et de Localisation Précise

Sigma0 Backscatter coefficient

SHM Safe Hold Mode

SSH Sea Surface Height

SSHA Sea Surface Height Anomalies

SLA Sea Level Anomaly

SLR Satellite Laser Ranging

SSR Solid State Recorder

SSB Sea State Bias

STD Standard Deviation

SWOT Surface Water Ocean Topography

SWH Significant Wave Height

TM TeleMetry

WTC Wet Tropospheric Correction

Table of Content

List of Figures

List of Tables

1 Introduction

Surface Water Ocean Topography (SWOT) is a joint project including NASA, Centre National d'Etudes Spatiales (CNES), the Canadian Space Agency and the UK Space Agency. The SWOT satellite carries onboard a wide-swath altimeter-interferometer in Ka-Band (KaRIn), a classical nadir-looking altimeter, as well as the usual complement on altimetry satellites: precise location systems and radiometer.

The SWOT Nadir Quality Assessment report are generated under SALP contract supported by CNES at the CLS Environment & Climate Business Unit. Cyclic assesment are made and are available on Aviso website.

A detailed description of the mission is available on AVISO website. Products description can be found in the SWOT Level-2 Nadir Altimeter products User Guide and dataset standards are described in SWOT Nadir user handbook.

The present document assesses SWOT Nadir data quality and mission performance **over ocean**.
After an executive summary in the following pages, dedicated sections of this report deal with:

- description of data processing,
- data coverage / availability,
- monitoring of rejected spurious data,
- analysis of relevant parameters derived from instrumental measurements and geophysical corrections,
- system performance via analyses at crossover points,
- system performance via along-track Sea Level Anomalies monitoring.

This document focus only on the operational 21-days orbit phase. A specific document is dedicated to the 1-day "calval" repetitive orbit phase. Thus, the period covered by this issue extends from cycle 001 (2023-07-21 09:44:23) to cycle 023 (2024-11-12 02:50:38) for Geophysical Data Record (GDR) and to cycle 025 (2024-12-23 20:20:46) for Interim Geophysical Data Record (IGDR).

2 Executive Summary

2.1. Data Availability

The behaviour of SWOT Nadir over ocean is good. In average SWOT Nadir provides 97.4% of measurements for GDR over 023 cycles and 97.45% for IGDR over 025 cycles.
A change in behavior is visible before and after September 12, 2023. Just after the orbit change to the Science phase, the altimeter parameters were not fully adapted to the new altitude, mainly affecting measurements at high latitudes. The data availability rate was slightly lower during this period, with missing data at latitudes greater than 66°. After the EEPROM update on September 12, 2023, the availability rate slightly increased. The data gap observed at the beginning of cycle 4 (September 21, 2023 to September 27, 2023) was due to an SSR stop caused by a power supply anomaly.

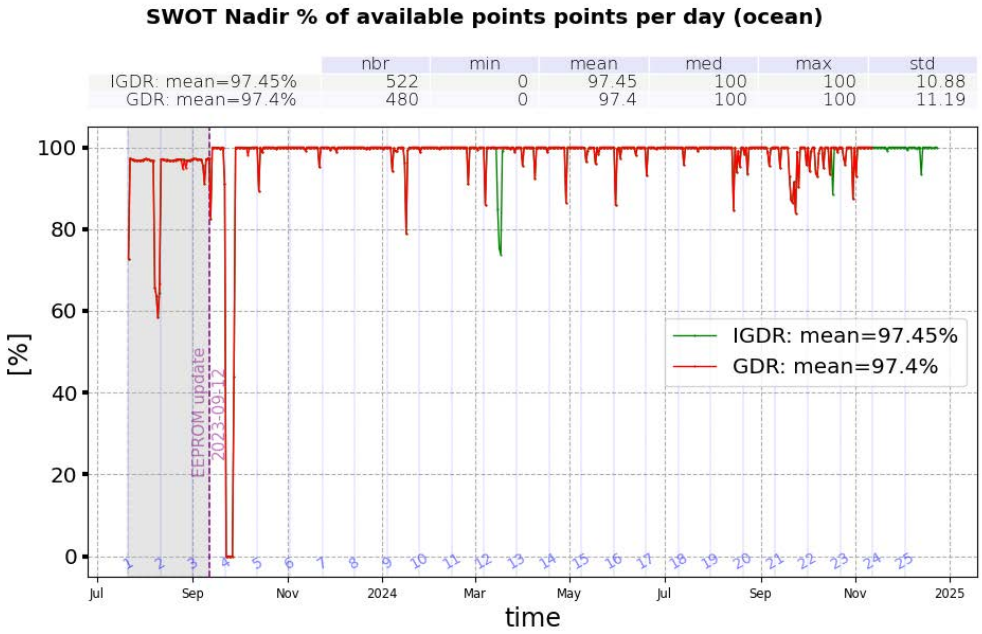

Figure 1: SWOT Nadir data availability over ocean (per day)

2.2. Data Validity

The average of total valid measurements over ocean is 82.54% (see Figure 2).
EEPROM update on 12 Sep. 2023 (C003) has a slight impact on edited data because more data near ice lands are available.
Over the 23 cycles, in average 14.79% of data were edited by ice over ocean. Over the studied period, no

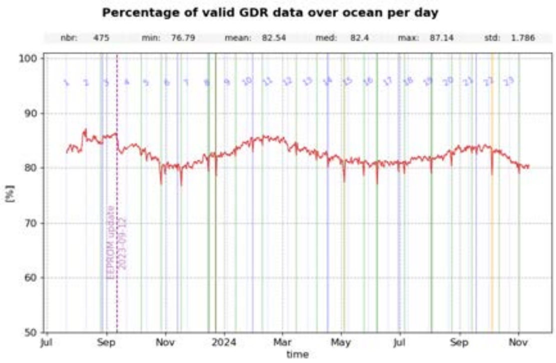

Figure 2: SWOT Nadir ocean data editing average by day.

anomalous trend is detected, only the annual seasonal signal is visible mainly due to ice coverage annual variations in north and south hemispheres.
After quality flag analysis, instrumental parameters have also been analyzed from comparison with thresholds.
The average of total edited measurements following threshold criterion is around 2.76% (Figure 3). Note that all outliers are on maneuver slots (colored lines).

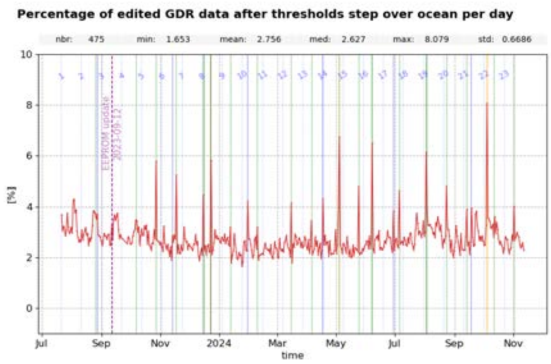

Figure 3: SWOT Nadir data editing by thresholds over ocean average by day.

2.3. Sea Wave Height

SWOT Nadir SWH is centered around 2.57 m for MLE4 (figure 4, top left). Comparison to ERA5 model shows a jump around cycle 10 that affects GDR and IGDR, it is linked to the introduction of Cryosat-2 in ERA5 model and it is also visible in other mission as Sentinel-6A-MF. The mean of differences tends to be higher after cycle 10 (figure 4, bottom left) while the standard deviation tends to be slightly reduced.

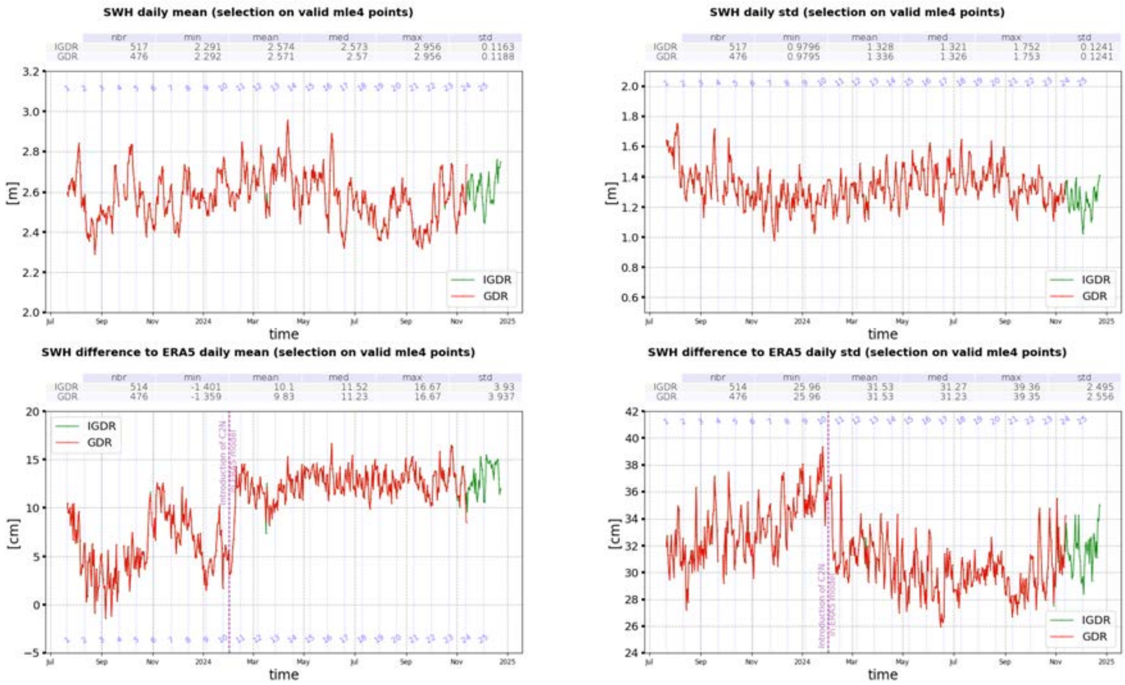

Figure 4: Monitoring of significant wave height

2.4. Wind Speed

For the current version of GDR, wind speed are not fitted to SWOT Nadir data, but the same biases as for Jason-3 GDR-F are applied. As a consequence, wind speed estimations are not aligned with ERA5 model in the GDR-F v1.04 version (figure 6).

The increase for IGDR of altimeter wind speed is explained by an update of the characterization file of the altimeter applied to IGDR from 2023-10-09 23:24:06 (Cycle 4 Pass 509). The daily average from cycle 001 to cycle 023 shows the wind speed values centered around 8.51 m/s for MLE4 (figure 5).

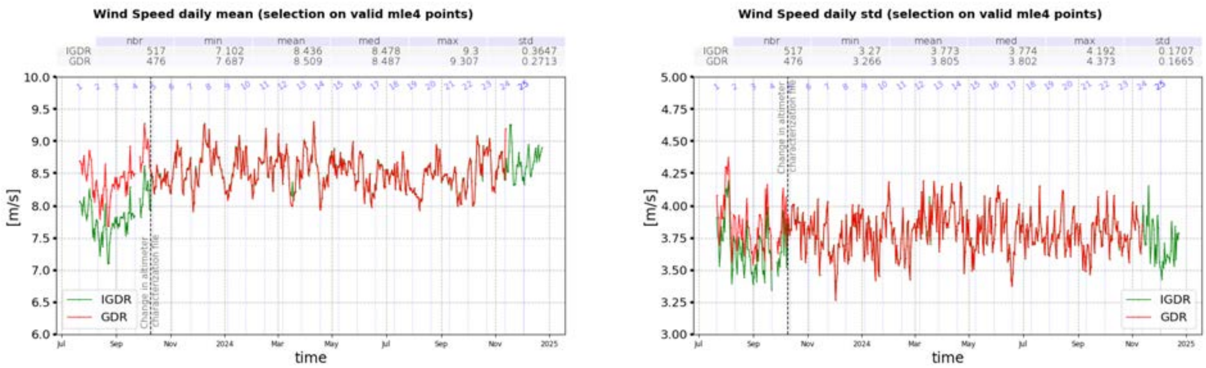

Figure 5: Monitoring of altimeter wind speed

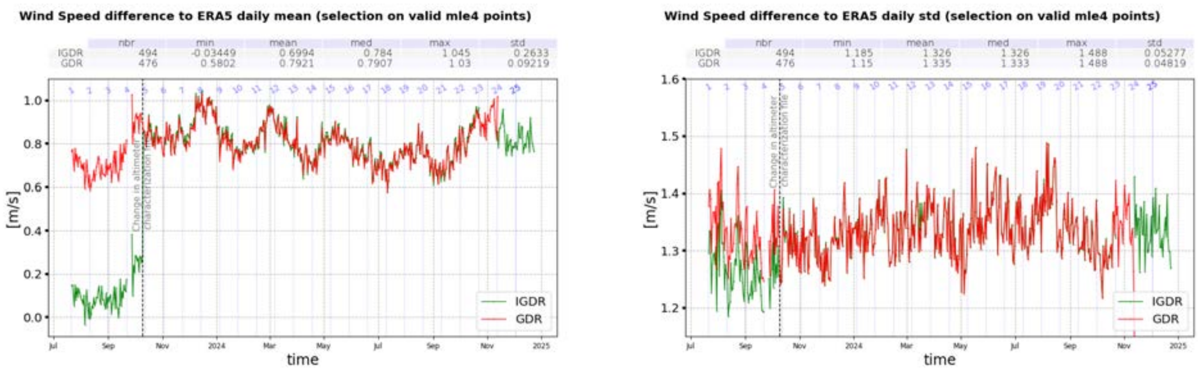

Figure 6: Monitoring of altimeter wind speed difference to ERA5 model

2.5. Sea Level Anomalies

SWOT Nadir shows an good stability in terms of SLA standard deviation.

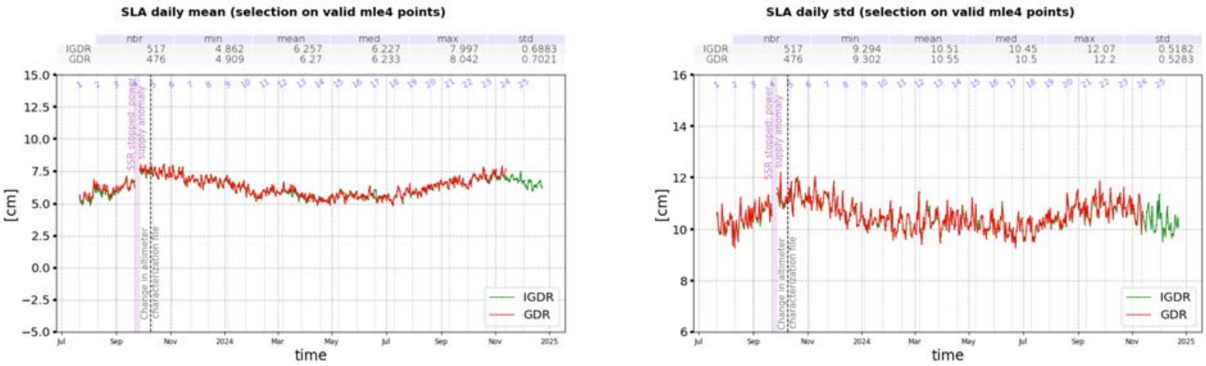

Figure 7: Cyclic monitoring of along-track SLA

2.6. Performances at crossover points

2.6.1. Monomission crossovers

Mean of Sea Surface Height (SSH) differences at crossovers is almost null showing the stability of measurements for this diagnostic. After data editing, applying additional geographical selection and SWOT Nadir standards, the crossover standard deviation for the period between cycle 001 and cycle 023 is about 5.03 cm in MLE4.

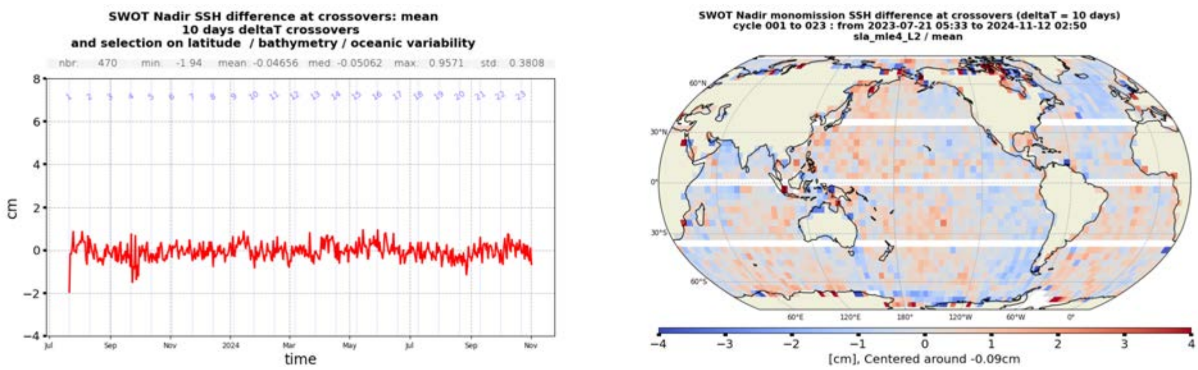

Figure 8: Mean SSH difference at crossovers

The daily standard deviation or variance of SSH crossovers differences are plotted in figure 9 after applying geographical criteria (bathymetry, latitude, oceanic variability).
This metric allows to estimate the system noise by dividing by $\sqrt{2}$ (which leads to 3.56 cm).

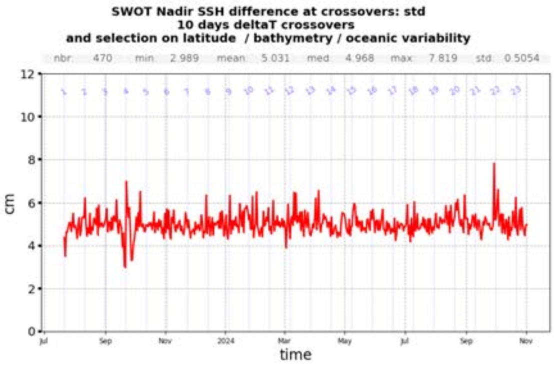

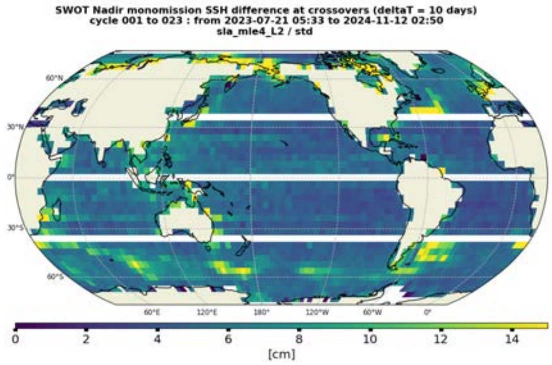

Figure 9: Std SSH difference at crossovers

2.6.2. Multimission crossovers

Mean SLA differences at SWOT Nadir/Sentinel-6A-MF crossovers is quite stable and around 1.015 cm in average. Figure 11 shows seasonal differences.

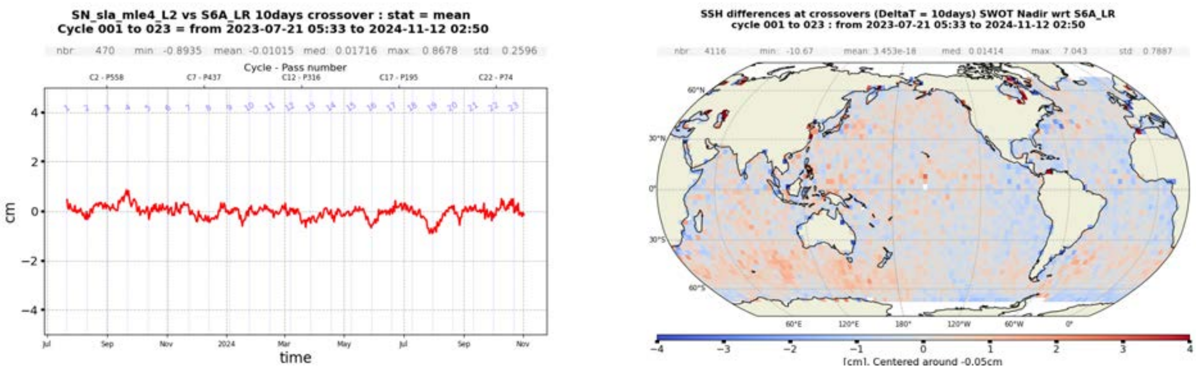

Figure 10: Mean SSH difference at crossovers between SWOT Nadir MLE4 and Sentinel-6 MF LR MLE4

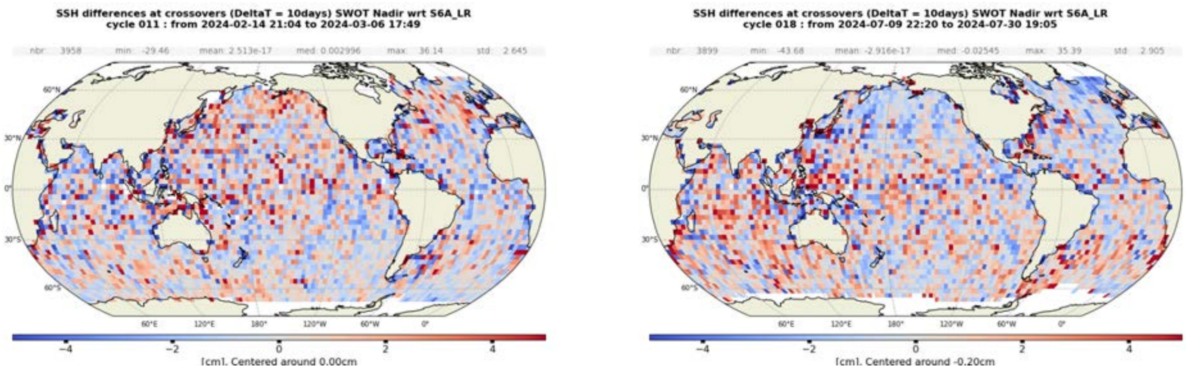

Figure 11: Mean SSH difference at crossovers between SWOT Nadir MLE4 and Sentinel-6 MF LR MLE4 for a winter cycle (left) and a summer cycle (right)

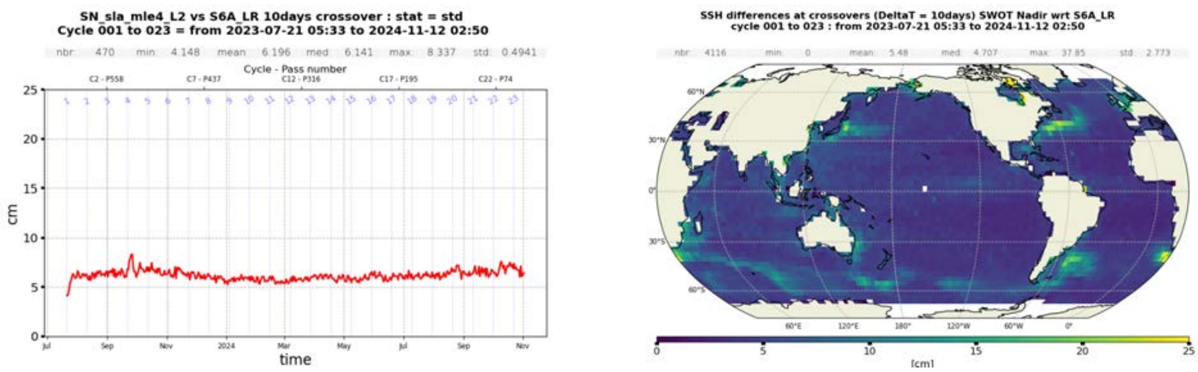

Figure 12: STD Daily monitoring of SSH difference at crossovers between SWOT Nadir MLE4 and Sentinel-6 MF LR MLE4

2.7. Known issues

Known issue: The current interpolation of radiometer data on the nadir track currently requires the two AMR sides to be defined and valid. When one AMR side is invalid (quality_flag_rad_wet_tropo_cor_qual), the nadir WTC can be affected by interpolation artifacts. Users who want to remove this subset of measurements can check the validity of the radiometer data and flags in the Radiometer L2 product (L2 RAD). In the next release, the SWOT Nadir processing will be updated to natively handle this border case: the radiometer flag (rad_wet_tropo_cor_interp_qual) in the L2 NALT will inform end-users of this degraded radiometer interpolation. In a future release, we plan to revisit the radiometer interpolation algorithm to mitigate or remove interpolation artifacts altogether.

Known issue: Users should also keep in mind that estimated wind speed has a 80cm bias with respect to the model until wind calibration is performed.

3 Processing Status

3.1. Data used

Metrics provided in this document are based on SWOT Nadir dataset from cycles 1 to 23 for GDR products (corresponding to July 07th 2023 to November 12th 2024). Note that all GDR data used in this report follow standard "F". IGDR's metrics are provided up to cycle 25 (up to December 23th 2024). Both IGDR and GDR data used are 1Hz data unless specified otherwise.

3.2. List of events

Table 1 shows the different maneuver types and their expected impact on data. Colored maneuvers affect data edited over the ocean, corresponding to the vertical lines in the temporal monitoring. As shown in Figure 13, GNC calibration mainly occurs on land and thus does not require a specific color. Only CALGYR_SLOT and YAWFLIP_SLOT (orange and blue lines) directly impact data validity. OCM_SLOT and NON_REF_ALT impact data availability and as a consequence validity statistics are affected.

Maneuver type	Expected impact
CALGYR_SLOT (gyroscope calibration)	Data rejected on editing criteria at DV on retracking and radiometer output variables
CNG Calibration (POSEIDON-3C in calibration mode)	Data unavailable
OCM_SLOT (burst for station keeping maneuver)	Data partially rejected or data unavailable
NON_REF_ALT (avoidance maneuver)	Data rejected or unavailable at the beginning and end of a maneuver in the burst period
SADM_CRUISE_SLOT (change of solar panel position)	No rejected data, no loss of coverage
YAWFLIP_SLOT (satellite flip-over)	Data rejected on editing criteria at DV on retracking and radiometer output variables

Table 1: Types of maneuvers and expected impacts

Table 2 shows the maneuvers during the Science phase of the SWOT Nadir mission.

Start Date	End Date	Cycle	Pass	Event Name
2023-08-15 09:15:24	2023-08-15 09:19:54	2	121	SADM_CRUISE_SLOT
2023-08-24 19:39:13	2023-08-24 19:43:43	2	385	SADM_CRUISE_SLOT
2023-08-25 20:43:57	2023-08-25 21:20:59	2	414	OCM_SLOT
2023-08-27 11:07:23	2023-08-27 11:29:52	2	459	YAWFLIP_SLOT
2023-08-30 12:52:07	2023-08-30 12:56:37	2	545	SADM_CRUISE_SLOT
2023-09-08 12:59:49	2023-09-08 13:04:19	3	213	SADM_CRUISE_SLOT
2023-10-06 17:13:26	2023-10-06 17:50:30	4	417	OCM_SLOT
2023-10-27 14:06:10	2023-10-27 14:43:12	5	417	OCM_SLOT
2023-11-02 15:56:04	2023-11-02 16:00:34	6	4	SADM_CRUISE_SLOT
2023-11-11 05:43:32	2023-11-11 05:48:02	6	244	SADM_CRUISE_SLOT
2023-11-13 19:28:23	2023-11-13 19:50:14	6	316	YAWFLIP_SLOT
2023-11-16 12:38:04	2023-11-16 12:42:34	6	392	SADM_CRUISE_SLOT
2023-11-17 10:54:05	2023-11-17 11:31:07	6	418	OCM_SLOT
2023-11-24 23:00:43	2023-11-24 23:05:13	7	44	SADM_CRUISE_SLOT
2023-12-15 21:28:44	2023-12-15 22:05:47	8	46	OCM_SLOT
2023-12-23 02:48:25	2023-12-23 03:25:39	8	248	OCM_SLOT
2023-12-23 03:25:39	2023-12-23 09:40:01	8	248	NON_REF_ALT
2023-12-23 09:40:01	2023-12-23 10:17:15	8	256	OCM_SLOT
2024-01-12 21:00:52	2024-01-12 21:37:55	9	245	OCM_SLOT

Start Date	End Date	Cycle	Pass	Event Name
2024-01-19 09:04:56	2024-01-19 09:09:26	9	427	SADM_CRUISE_SLOT
2024-01-27 17:42:51	2024-01-27 17:47:21	10	77	SADM_CRUISE_SLOT
2024-01-30 07:27:39	2024-01-30 07:50:26	10	149	YAWFLIP_SLOT
2024-02-02 00:37:24	2024-02-02 00:41:54	10	225	SADM_CRUISE_SLOT
2024-02-09 17:50:40	2024-02-09 18:27:43	10	441	OCM_SLOT
2024-02-10 11:00:51	2024-02-10 11:05:21	10	461	SADM_CRUISE_SLOT
2024-03-15 21:10:32	2024-03-15 21:47:35	12	256	OCM_SLOT
2024-04-05 08:48:44	2024-04-05 08:53:24	13	246	SADM_CRUISE_SLOT
2024-04-05 17:40:48	2024-04-05 18:17:51	13	256	OCM_SLOT
2024-04-14 05:28:48	2024-04-14 05:33:28	13	494	SADM_CRUISE_SLOT
2024-04-17 02:05:41	2024-04-17 02:27:40	13	574	YAWFLIP_SLOT
2024-04-19 22:41:42	2024-04-19 22:46:22	14	70	SADM_CRUISE_SLOT
2024-04-29 05:41:30	2024-04-29 05:46:10	14	330	SADM_CRUISE_SLOT
2024-05-03 21:14:17	2024-05-03 21:51:21	14	460	OCM_SLOT
2024-05-04 12:40:02	2024-05-04 21:43:01	14	478	CALGYR_SLOT
2024-05-24 19:26:13	2024-05-24 20:03:17	15	462	OCM_SLOT
2024-06-07 08:21:55	2024-06-07 08:59:17	16	257	OCM_SLOT
2024-06-07 17:47:45	2024-06-07 18:25:06	16	268	OCM_SLOT
2024-06-17 03:16:33	2024-06-17 03:21:13	16	530	SADM_CRUISE_SLOT
2024-06-26 13:39:55	2024-06-26 13:44:35	17	211	SADM_CRUISE_SLOT
2024-06-29 10:16:38	2024-06-29 10:38:58	17	291	YAWFLIP_SLOT
2024-07-02 05:09:28	2024-07-02 05:14:08	17	369	SADM_CRUISE_SLOT
2024-07-05 19:02:56	2024-07-05 19:40:00	17	469	OCM_SLOT
2024-07-11 01:50:16	2024-07-11 01:54:56	18	33	SADM_CRUISE_SLOT
2024-08-02 20:45:31	2024-08-02 21:22:34	19	86	OCM_SLOT
2024-08-23 20:50:00	2024-08-23 21:27:04	20	90	OCM_SLOT
2024-09-06 23:51:30	2024-09-06 23:56:10	20	486	SADM_CRUISE_SLOT
2024-09-13 20:45:28	2024-09-13 21:22:33	21	94	OCM_SLOT
2024-09-15 10:12:17	2024-09-15 10:16:57	21	138	SADM_CRUISE_SLOT
2024-09-17 23:57:00	2024-09-18 00:18:56	21	210	YAWFLIP_SLOT
2024-09-20 15:23:44	2024-09-20 15:28:24	21	284	SADM_CRUISE_SLOT
2024-09-29 00:03:33	2024-09-29 00:08:13	21	518	SADM_CRUISE_SLOT
2024-10-04 10:25:57	2024-10-04 19:28:56	22	86	CALGYR_SLOT
2024-10-11 13:51:14	2024-10-11 14:28:18	22	286	OCM_SLOT
2024-11-01 07:00:01	2024-11-01 07:37:06	23	281	OCM_SLOT
2024-11-15 18:49:49	2024-11-15 19:26:52	24	103	OCM_SLOT
2024-11-25 18:37:34	2024-11-25 18:42:14	24	383	SADM_CRUISE_SLOT
2024-12-03 16:59:06	2024-12-03 17:03:46	25	21	SADM_CRUISE_SLOT
2024-12-06 04:56:38	2024-12-06 05:33:41	25	91	OCM_SLOT
2024-12-06 10:09:59	2024-12-06 10:32:45	25	97	YAWFLIP_SLOT
2024-12-09 05:02:56	2024-12-09 05:07:36	25	175	SADM_CRUISE_SLOT
2024-12-18 06:53:45	2024-12-18 06:58:25	25	429	SADM_CRUISE_SLOT
2024-12-20 21:40:50	2024-12-20 22:17:52	25	502	OCM_SLOT

Table 2: Maneuvers on Science Phase SWOT Nadir mission.

Table 3 lists the POSEIDON-3C (POS-3C) CNG calibrations during the Science phase of the SWOT Nadir mission. Note that this type of calibration always lasts 33 minutes and 3 seconds.
The corresponding locations of POS-3C CNG calibrations can be found in figure 13.

Start Date	End Date	Cycle	Pass
18/09/2023 18:22:00	18/09/2023 18:55:03	3	499
21/12/2023 03:44:00	21/12/2023 04:17:03	8	193
23/03/2024 13:07:00	23/03/2024 13:40:03	12	471
25/06/2024 22:30:00	25/06/2024 23:03:03	17	193
07/09/2024 11:07:00	07/09/2024 11:40:03	20	499
10/12/2024 20:30:00	10/12/2024 21:03:03	25	221

Table 3: POS-3C Calibration (CNG) on Science Phase SWOT Nadir mission.

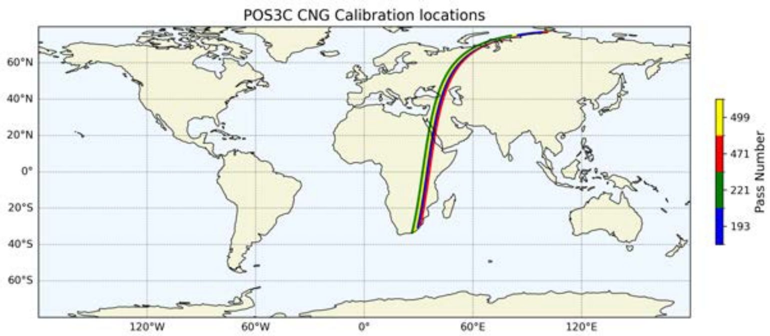

Figure 13: Different POS-3C CNG calibration locations

Other events that impact data availability occured for the period are listed in this table:

Start Date	End Date	Cycle	Pass	Event Type
2023-09-21 22:13:00	2023-09-27 08:33:00	4	3-162	SSR stopped
2023-10-08 17:12:02	18:53:14	4	473-475	SSR anomaly
2023-10-13 00:29:50	02:39:22	5	10-12	SSR anomaly
2023-10-13 10:20:30	12:22:02	5	21-24	SSR anomaly
2023-11-14 17:52:06	19:36:58	6	342-344	SSR anomaly
2024-02-25 00:35:00	03:17:00	11	284-288	SSR anomaly
2024-03-02 14:28:00	16:21:00	11	469-471	SSR anomaly
2024-03-07 04:59:00	06:57:00	12	14-16	SSR anomaly
2024-05-04 12:20:02	21:43:01	14	477-488	Gyroscope calibration
2024-05-12 23:10:56	23:22:24	15	130	SSR anomaly
2024-05-19 01:49:15	03:24:30	15	301-303	SSR anomaly
2024-10-04 10:25:57	19:28:56	22	86-96	Gyroscope calibration
2024-10-11 13:36:00	15:21:00	22	285-287	SSR BIOS update
2024-10-24 09:42:46	10:28:10	23	61-62	EDAC error

Table 4: Other Events on Science Phase SWOT Nadir mission.

3.3. Tracking and acquisition mode

SWOT Nadir is able to track data with several onboard tracker modes: POSEIDON-3C instrument implements three main tracking modes:

- The autonomous acquisition and tracking mode (M1)
- The DIODE acquisition and autonomous tracking mode (M2)
- The DIODE & DEM mode (M3)

and certain automatic transitions can also be authorized by the user, as is the case in M4 to M4bis modes. The different tracking modes are described in the article of Guérin *et al.* [23]. The status of tracking and acquisition modes are detailed in table 5. The acquisition mode as shown correponds to the netcdf field *alt_state_acq_mode_flag* which is the 20Hz altimeter state flag.

Cycle	Acquisition Mode
Cycle 001 to cycle 004 until 2023-10-09	Autonomous acquisition and tracking mode (M1)
Cycle 004 since 2023-10-09 to cycle 023	DIODE + DEM tracking with automatic transition and direct transition from Open Loop to Closed Loop (M4bis mode)

Table 5: SWOT Nadir Acquisition Mode.

- From cycle 001 to cycle 004 (until 2023-10-09), autonomous acquisition and tracking mode was activated (fig. 14).

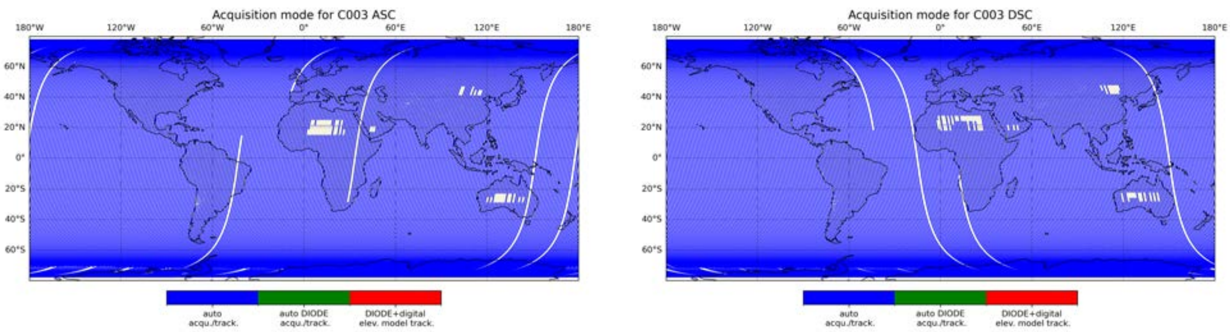

Figure 14: Acquisition mode (for cycle 003. 8 = autonomous acquisition / tracking, 9 = autonomous DIODE acquisition / tracking, 10 = DIODE + Digital Elevation Model tracking

- From cycle cycle 004 (since 2023-10-09) to cycle 023, DIODE + DEM tracking with auto transition and direct transition from Open Loop to Close Loop mode was activated (fig. 15).

Over the considered period, autonomous tracking mode (which comes from the L2 field *alt_state_track_trans_flag*) for SWOT Nadir is always authorized.

3.4. Models and standards

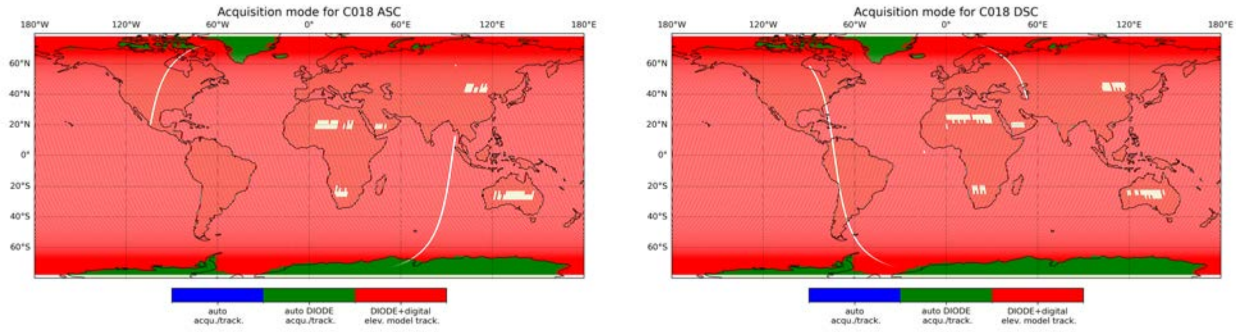

Figure 15: Acquisition mode for cycle 018. 8 = autonomous acquisition / tracking, 9 = autonomous DIODE acquisition / tracking, 10 = DIODE + Digital Elevation Model tracking

The period between cycle 001 and cycle 023, for GDR only, has been produced with the Processing Baseline F v1.04, and the processing software references L1 library=V5.8.4 and L2 library=V6.10p1p2p3p4p5. Processing Pilot for IGDR and GDR change within the period:

Processing Pilot	IGDR	GDR
5.0.4	C001 to C005/P092	/
5.1.0	C005/P093 to C022/P352	C001 to C019
5.2.4	C022/P353 to C025	C020 to C023

Table 6: Processing Pilot version

The standard "F" definition is given in the Jason-3 user handbook.

3.5. Missing measurements

3.5.1. Over land and ocean

Determination of missing measurements relative to the theoretically expected orbit ground pattern is an essential tool to detect missing telemetry or satellite events for instance. Figure 16 shows the percentage of available measurements for SWOT Nadir for all kinds of surfaces observed, computed with respect to a theoretical possible number of measurements. In average SWOT Nadir provides 96.7% of measurements for GDR over 023 cycles and 96.74% for IGDR over 025 cycles. Note that for the same period as GDR, 96.53% of IGDR measurements are available globally.

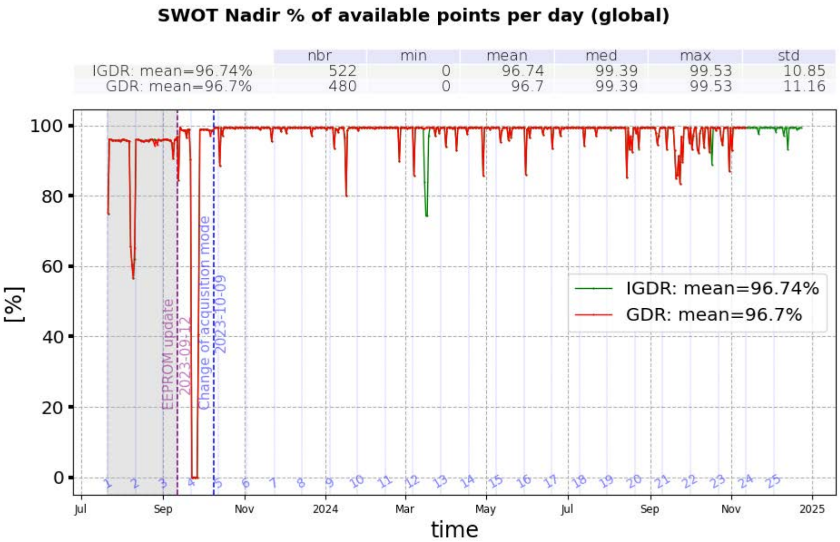

Figure 16: Global data availability per day

A change of behaviour is visible before and after the 12 Sep. 2023 because just after the orbit change to Science phase, altimeter parameters file was not completely adapted to the new altitude, which mainly impacted the ability to take measurements at high latitudes. The availability rate of data is then slightly lower over this period (light gray on figure 16), with missing data located at |latitude|>66°. After the EEPROM update the 12 Sep. 2023, the availability rate is slightly higher (Figure 17).
A second slighter change of behaviour is visible after the 10 Oct. 2023 and linked to the change of acquisition mode from M1 to M4bis (as described in section 3.3.). This evolution makes data availability slightly better on hydrology targets because of the use of a Digital Elevation Model (DEM). As a result, the impact is not significant on ocean statistics but only on global ones.

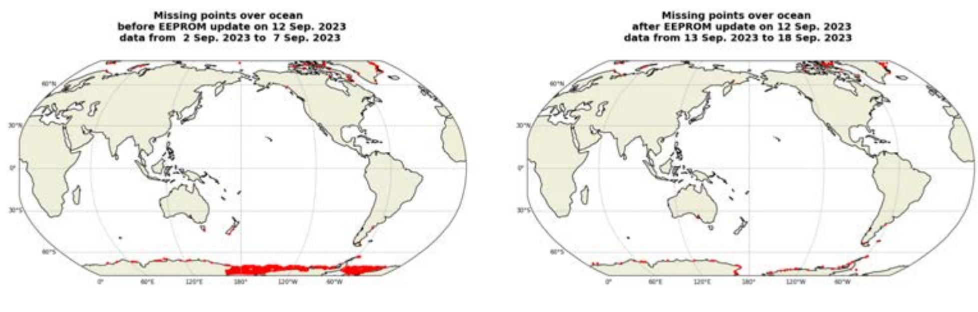

Figure 17: Missing points over ocean before and ater EEPROM update

The consequent data gap observed at the begining of cycle 4 (2023-09-21 21:34:07 to 2023-09-27 14:42:40) is explained by a Solid State Recorder (SSR) stop because of a power supply anomaly.

3.5.2. Over ocean

The selection over ocean is applied regarding the L2 surface type flag. The behaviour of SWOT Nadir over ocean is good. In average SWOT Nadir provides 97.4% of ocean measurements over 23 cycles for GDR and 97.45% for IGDR over 25 cycles (figure 18). Note that for the same period as GDR, 97.24% of IGDR measurements are available over ocean.

Looking at data over ocean, SWOT Nadir is nearly always available (ocean is fully covered) out of specific events (see figure 18).

As for figure 16, the EEPROM update on 12 Sep. 2023 allows the availability rate to be slightly higher with a better availability rate over |latitude|>66°.

The consequent data gap observed at the begining of cycle 4 (2023-09-21 21:34:07 to 2023-09-27 14:42:40) is explained by a SSR stop because of a power supply anomaly.

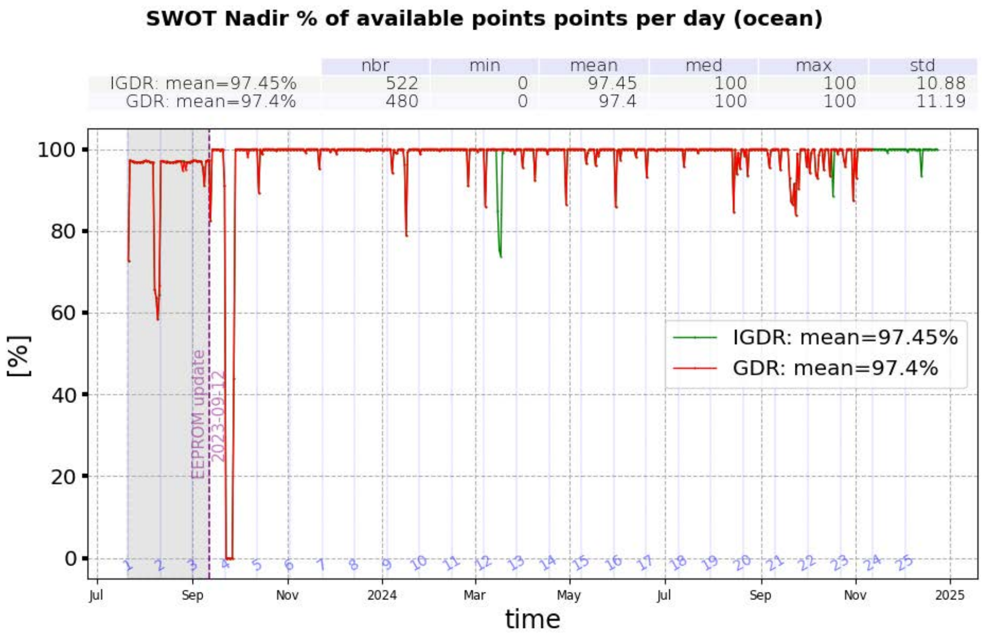

Figure 18: SWOT Nadir data availability over ocean (per day)

Table 7 lists all the data gap over ocean for the period between cycles 001 and 023.

Cycle	Start	End	Details
C001	2023-07-21 05:35:38	2023-07-21 09:44:22	Impacting passes 1 to 5 with respectively 100.00%, 100.00%, 100.00%, 100.00% and 82.07% over ocean.
C001	2023-08-07 14:01:02	2023-08-07 21:40:46	Impacting passes 486 to 495 with respectively 52.13%, 100.00%, 67.45%, 100.00%, 100.00%, 100.00% and 89.93% over ocean due to connection loss with IVK.

Cycle	Start	End	Details
C001	2023-08-08 14:01:46	2023-08-08 21:40:41	Impacting passes 514 to 523 with respectively 51.73%, 100.00%, 65.55%, 100.00%, 100.00%, 100.00%, 100.00%, 100.00%, 100.00% and 89.57% over ocean due to connection loss with IVK.
C001	2023-08-09 09:08:52	2023-08-09 22:05:39	Impacting passes 537 to 551 with respectively 90.77%, 53.95%, 71.32%, 100.00%, 44.52%, 77.09%, 100.00%, 100.00%, 100.00%, 58.28%, 100.00%, 100.00% and 100.00% over ocean due to connection loss with IVK.
C001	2023-08-10 23:56:41	2023-08-11 20:23:33	Impacting passes 554, 555 and 570 to 577 with respectively 77.94%, 62.77%, 63.48% ,100.00%, 66.86%, 100.00% ,100.00%, 100.00%, 100.00% and 100.00% over ocean due to connection loss with IVK.
C002	2023-08-25 20:53:44	2023-08-25 21:17:57	Impacting passes 414 to 415 with respectively 47.71% and 2.55% of missing data over ocean due to OCM SLOT.
C002	2023-08-27 11:06:14	2023-08-27 11:47:52	Pass 459 : 42.97% over ocean due to YAW FLIP.
C003	2023-09-07 23:10:34	2023-09-08 01:20:37	Due to KUX Pass loss (impacting pass 197 to 199 with respectively 31.04%, 100.00% and 49.87% over ocean).
C003	2023-09-12 09:04:29	2023-09-12 12:21:43	Due to Poseidon in stand-by mode (impacting pass 320 to 324 with respectively 64.63%, 100.00%, 100.00%, 100.00% and 41.48% over ocean).
C003	2023-09-18 18:36:43	2023-09-18 18:55:03	Pass 499 : 22.71% over ocean due to POS-3C calibration CNG step.
C004	2023-09-21 21:34:07	2023-09-27 14:42:40	Due to SSR stop because of power supply anomaly (impacting 59.46% of pass 003, 100% of passes 004 to 161 and 13.48% of pass 162, of missing data over ocean).
C004	2023-10-06 17:23:08	2023-10-06 17:46:03	Pass 418 : 42.02% over ocean due to OCM SLOT.
C005	2023-10-13 01:16:41	2023-10-13 03:42:55	Due to double edac on ssr (impacting passes 11 to 14 with respectively 81.59%, 100.00%, 100.00% and 22.35% of missing data over ocean).
C005	2023-10-13 12:21:05	2023-10-13 12:21:33	Pass 24 : 1.12% over ocean (<1min).
C005	2023-10-15 10:10:50	2023-10-15 10:35:30	Due to file too small (impacting passes 77 to 78 with respectively 23.10% and 13.77% of missing data over ocean).
C005	2023-10-15 23:14:12	2023-10-15 23:14:55	Pass 092 : 2.64 % over ocean (<1min)
C005	2023-10-21 08:54:49	2023-10-21 08:55:10	Pass 243 : 1.18 % over ocean (<1min)
C005	2023-10-24 19:36:59	2023-10-24 19:39:43	Pass 340 : 10.06 % over ocean due to SWOT CREX L0A/DORIS/1178 DOPPLER.
C005	2023-10-28 19:41:39	2023-10-28 19:41:49	Pass 452 : 0.56 % over ocean (<1min)

Cycle	Start	End	Details
C006	2023-11-12 17:19:02	2023-11-12 17:29:49	Impacting pass 285 with 22.23% due to Doris/-Doppler anomalies.
C006	2023-11-21 07:35:12	2023-11-21 08:35:36	Impacting passes 526 to 527 with respectively 83.78% and 57.50% due to KRX station anomalies.
C007	2023-11-28 10:53:50	2023-11-28 10:59:52	Impacting passes 141 to 142 with respectively 13.67% and 3.50% due to several missing segments.
C007	2023-11-30 22:59:36	2023-11-30 22:59:41	Impacting pass 212 with 0.20% due to missing points at high latitude.
C007	2023-12-02 00:49:49	2023-12-02 01:05:33	Pass 242: 41.24 % (several segments over ocean)
C007	2023-12-04 08:14:56	2023-12-04 08:15:09	Pass 306: 0.54 % (in Southern Pacific)
C007	2023-12-12 23:25:46	2023-12-12 23:26:07	Pass 548: 0.74 % (11 non continuous points in Carribean sea)
C008	2023-12-21 03:44:01	2023-12-21 04:17:02	Pass 193 : 21.54% over ocean (CNG calibration).
C008	2023-12-23 11:01:40	2023-12-23 11:05:39	Pass 257 : 8.81% over ocean.
C008	2024-01-01 11:05:09	2024-01-01 11:10:06	Pass 509 : 6.62% over ocean (Ground station anomaly).
C009	2024-01-07 21:48:23	2024-01-07 22:27:49	Pass 106 : 86.23% over ocean (altimeter TM loss).
C009	2024-01-07 22:27:50	2024-01-07 23:12:44	Pass 107 : 89.91% over ocean (altimeter TM loss).
C009	2024-01-08 18:43:47	2024-01-08 18:50:44	Pass 130 : 5.45% over ocean (multiple PLM gaps).
C009	2024-01-08 19:17:43	2024-01-08 19:17:50	Pass 131 : 0.62% over ocean (multiple PLM gaps).
C009	2024-01-09 15:12:17	2024-01-09 15:14:07	Pass 154 : 5.81% over ocean (multiple PLM gaps on IVK).
C009	2024-01-09 16:40:03	2024-01-09 16:43:29	Pass 156 : 7.85% over ocean (multiple PLM gaps on IVK).
C009	2024-01-09 18:16:40	2024-01-09 18:28:28	Pass 158 : 11.25% over ocean (multiple PLM gaps on IVK).
C009	2024-01-10 09:27:04	2024-01-10 09:33:52	Pass 175 : 6.56% over ocean (multiple PLM gaps, strong winds over Kiruna).
C009	2024-01-10 15:15:39	2024-01-10 15:19:19	Pass 182 : 10.66% over ocean (multiple PLM gaps on IVK).
C009	2024-01-:46:23	2024-01-10 16:50:00	Pass 184 : 8.15% over ocean (multiple PLM gaps on IVK).
C009	2024-01-10 19:27:23	2024-01-10 19:27:39	Pass 187 : 0.96% over ocean (multiple PLM gaps on IVK).
C009	2024-01-15 23:14:06	2024-01-15 23:23:25	Pass 331 : 7.16% over ocean (SSR error).
C009	2024-01-15 23:23:26	2024-01-16 04:32:05	Passes 332 to 337 : 100% over ocean (SSR error).
C009	2024-01-16 04:32:06	2024-01-16 05:06:01	Pass 338 : 7.80% over ocean (SSR error).

Cycle	Start	End	Details
C009	2024-01-17 14:41:38	2024-01-17 14:42:06	Pass 377 : 1.10% over ocean (SSR error).
C009	2024-01-17 18:30:10	2024-01-17 18:38:45	Pass 382 : 27.36% over ocean (PLTM gaps between 2 successive dumps).
C009	2024-01-19 10:05:43	2024-01-19 10:06:19	Pass 428 : 2.15% over ocean (multiple PLM gaps).
C010	2024-01-25 22:11:59	2024-01-25 22:23:39	Pass 026 : 25.28% over ocean (PLTM gap).
C010	2024-01-25 22:55:03	2024-01-25 23:27:30	Pass 027 : 3.59% over ocean (PLTM gap).
C010	2024-02-06 18:22:55	2024-02-06 18:25:37	Pass 357 : 9.63% over ocean (PLTM gap).
C010	2024-02-07 12:43:49	2024-02-07 13:17:52	Pass 379 : 0.05% over ocean.
C011	2024-02-25 01:01:36	2024-02-25 03:17:13	Due to SSR anomaly (impacting passes 285 to 288 with respectively 43.19%, 100%, 100% and 15.13% of missing data over ocean).
C011	2024-03-02 14:38:27	2024-03-02 14:43:10	Pass 469 : 15.51% over ocean (SSR anomaly) over Indian ocean.
C011	2024-03-02 16:21:11	2024-03-02 16:21:39	Pass 471 : 2.77% over ocean (SSR anomaly) near eastern coast of South Africa.
C012	2024-03-07 05:02:45	2024-03-07 08:16:33	Due to SSR anomaly : impacting passes 014 to 017, with respectively 99.26%, 100.00%, 100.00% and 86.55% of missing data over ocean
C012	2024-03-10 21:48:46	2024-03-10 21:49:15	Pass 117: 1.82% of missing ocean data over ocean (<1min)
C012	2024-03-14 08:50:40	2024-03-14 08:51:35	Pass 214: 1.44% of missing ocean data over ocean (<1min)
C012	2024-03-15 22:10:57	2024-03-15 22:11:38	Impacting passes 257 to 258, with respectively 1.75% and 0.35% of missing ocean data over ocean
C012	2024-03-23 13:20:44	2024-03-23 13:37:56	Pass 471: 20.80 % of missing data over ocean
C012	2024-03-26 06:58:04	2024-03-26 07:14:00	Pass 548: 41.40% of missing data over ocean due to Antenna station issue (KUX)
C013	2024-03-27 23:45:38	2024-03-27 23:45:41	Pass 011 : 0.19 % over ocean (< 1min)
C013	2024-03-31 07:02:18	2024-03-31 08:24:52	Due to Alti PLTM not received (impacting passes 104 to 105 with respectively 78.66 % and 87.00 % of missing data over ocean)
C013	2024-04-08 00:24:11	2024-04-08 01:49:14	Due to PLTM not received (impacting passes 320 to 322 with respectively 61.53 %, 100.00 % and 41.24 % of missing data over ocean)
C013	2024-04-16 18:43:14	2024-04-16 19:08:47	Impacting passes 565 to 566 with respectively 19.22 % and 15.69 % of missing data over ocean
C014	2024-04-18 01:16:23	2024-04-18 01:16:43	Pass 017 : 0.44% over ocean (<1min).
C014	2024-04-25 14:09:55	2024-04-25 14:31:33	Pass 228 : 5.72% over ocean.
C014	2024-04-28 05:02:05	2024-04-28 08:18:45	Due to cancelled downlink (impacting passes 301 to 305 with respectively 12.46%, 100.00%, 100.00%, 100.00% and 64.12% of missing data over ocean).

Cycle	Start	End	Details
C014	2024-04-28 17:46:17	2024-04-28 17:46:17	Pass 316 : 1.68% over ocean (<1min).
C015	2024-05-10 07:06:29	2024-05-10 07:20:29	Impacting passes 055 to 056 with respectively 2.22% and 1.03% of missing data over ocean.
C015	2024-05-11 10:55:01	2024-05-11 11:56:34	Impacting passes 088 to 089 with respectively 91.20% and 23.53% of missing data over ocean due to station or network issue.
C015	2024-05-12 23:10:19	2024-05-12 23:21:56	Pass 130 : 22.29% over ocean due to SSR anomaly.
C015	2024-05-15 13:25:39	2024-05-15 13:26:20	Pass 203 : 1.84% over ocean.
C015	2024-05-17 10:55:31	2024-05-17 11:54:58	Impacting passes 256 to 257 with respectively 86.94% and 49.59% of missing data over ocean due to PLTM gap.
C015	2024-05-19 01:49:08	2024-05-19 02:24:29	Impacting passes 301 to 302 with respectively 12.39% and 18.81% of missing data over ocean due to SSR anomaly.
C015	2024-05-19 09:38:35	2024-05-19 09:46:23	Pass 310 : 15.74% over ocean.
C016	2024-05-30 11:10:29	2024-05-30 14:16:24	Impacting pass 036 to 039 with respectively 84.64%, 100.00%, 100.00% and 100.00% of missing data over ocean, due to SSR anomaly.
C016	2024-05-30 18:49:12	2024-05-30 19:24:10	Pass 045 : 13.10% over ocean.
C016	2024-05-31 07:30:39	2024-05-31 07:59:20	Pass 060 : 10.18% over ocean.
C016	2024-05-31 14:33:36	2024-05-31 14:56:36	Pass 068 : 2.08% over ocean due to SSR anomaly.
C016	2024-06-02 15:56:13	2024-06-02 16:38:26	Impacting pass 125 to 126 with respectively 7.54% and 70.46% of missing data over ocean, due to PLTM lost.
C016	2024-06-12 17:14:50	2024-06-12 18:08:53	Impacting pass 407 to 408 with respectively 15.73% and 38.43% of missing data over ocean due to SSR anomaly.
C016	2024-06-16 22:59:42	2024-06-16 22:59:52	Pass 526 : 0.41% over ocean.
C017	2024-06-19 14:44:00	2024-06-19 16:10:18	Pass 016 to 018 with respectively 67.61%, 99.32% and 1.58% over ocean, multiple gaps.
C017	2024-06-25 22:30:01	2024-06-25 23:03:02	Pass 193 : 23.10% over ocean due to POS-3C calibration CNG steps.
C017	2024-06-27 02:37:39	2024-06-27 03:05:30	Pass 226 : 4.03% over ocean (<1min).
C017	2024-07-08 18:09:57	2024-07-08 18:13:52	Pass 552 : 0.81% over ocean.
C018	2024-07-10 11:36:36	2024-07-10 11:37:08	Pass 016 : 1.32% over ocean.
C018	2024-07-13 14:47:29	2024-07-13 16:10:16	Pass 104 to 105 with respectively 79.69% and 83.31% over ocean due to alti data not received.
C018	2024-07-22 04:06:30	2024-07-22 04:41:29	Pass 343 to 344 with respectively 13.85% and 15.17% over ocean due to IVK downlink not received.
C019	2024-08-04 06:57:10	2024-08-04 06:57:51	Pass 126 : 1.63% over ocean.
C019	2024-08-09 02:57:05	2024-08-09 02:57:08	Pass 262 : 0.28% over ocean.

Cycle	Start	End	Details
C019	2024-08-14 13:07:04	2024-08-14 14:47:55	Pass 413 to 415 : 10.10%, 100.00% and 88.29% of missing data over ocean due to data distribution anomaly.
C019	2024-08-14 16:17:56	2024-08-14 18:15:57	Pass 417 to 419 : 20.15%, 100.00% and 86.21% of missing data over ocean due to data distribution anomaly.
C019	2024-08-16 11:42:49	2024-08-16 13:11:01	Pass 468 to 469 : 86.63% and 92.77% of missing data over ocean due to HBX Antenna issue.
C019	2024-08-17 11:13:41	2024-08-17 11:47:36	Pass 495 to 496 : 9.94% and 13.48% of missing data over ocean due to HBX Antenna issue.
C019	2024-08-18 11:15:34	2024-08-18 12:05:07	Pass 523 to 524 : 10.60% and 56.02% of missing data over ocean due to HBX Antenna issue.
C019	2024-08-18 21:22:42	2024-08-18 22:11:57	Pass 535 to 536 : 46.79% and 23.90% of missing data over ocean due to KRB downlink not received.
C020	2024-08-21 01:44:33	2024-08-21 02:07:09	Pass 012 : 63.80% over ocean due to IVK antenna tracking anomaly.
C020	2024-08-23 03:17:57	2024-08-23 04:38:10	Passes 070 to 071 : 73.61% and 91.43% of missing data over ocean due to IVK antenna tracking anomaly.
C020	2024-08-24 05:52:17	2024-08-24 06:25:23	Pass 101 : 1.48% over ocean due to SSR anomaly.
C020	2024-09-06 23:35:24	2024-09-06 01:11:19	Passes 457 to 459 : 4.83%, 100.00% and 91.43% of missing data over ocean due to IVK incomplete distribution - band X programming issue.
C020	2024-09-07 11:07:00	2024-09-07 11:40:02	Pass 499 : 15.02% over ocean due to SWOT/-POS Special calibrations (CAL1 CNG).
C021	2024-09-13 03:43:10	2024-09-13 05:00:01	Passes 074 to 076 : 43.42%, 100.00% and 17.08% of missing data over ocean due to data loss.
C021	2024-09-19 06:55:29	2024-09-19 08:32:25	Passes 246 to 248 : 87.93%, 100.00% and 12.64% of missing data over ocean due to alti data not received.
C021	2024-09-20 04:43:53	2024-09-20 06:21:58	Passes 271 to 273 : 12.65%, 100.00% and 87.59% of missing data over ocean due to data loss.
C021	2024-09-20 15:19:22	2024-09-20 17:16:07	Passes 284 to 286 : 86.68 %, 100.00 and 12.72 % of missing data over ocean due to KRX data not received.
C021	2024-09-21 15:27:03	2024-09-21 17:49:07	Passes 312 to 314 : 66.74 %, 100.00 and 14.27 % of missing data over ocean due to KRX data not received.
C021	2024-09-21 18:30:24	2024-09-21 20:11:11	Passes 315 to 317 : 14.28 %, 100.00 and 92.00 % of missing data over ocean due to KRX data not received.
C021	2024-09-22 04:44:56	2024-09-22 05:06:57	Passes 327 to 328 : 13.58 % and 13.47 % of missing data over ocean due to IVK HDX issue.

Cycle	Start	End	Details
C021	2024-09-22 06:35:25	2024-09-22 08:06:45	Passes 329 to 331 : 11.66 %, 100.00 and 92.78 % of missing data over ocean.
C021	2024-09-22 23:52:56	2024-09-22 2024-09-	Passes 350 to 352 : 96.32 %, 100.00 and 6.34 % of missing data over ocean due to antenna issue.
C021	2024-09-23 04:36:17	2024-09-23 05:10:59	Passes 355 to 356 : 15.08 % and 14.06 % of missing data over ocean due to COR Anomaly.
C021	2024-09-23 06:30:58	2024-09-23 08:11:23	Passes 357 to 359 : 11.39 %, 100.00 and 91.60 % of missing data over ocean due to data loss.
C021	2024-09-24 16:41:43	2024-09-24 17:17:59	Passes 397 to 398 : 15.45 % and 18.24 % of missing data over ocean to data loss (some APID)
C021	2024-09-25 05:12:31	2024-09-25 06:29:17	Passes 412 to 413 : 85.94 % and 89.79 % of missing data over ocean to data loss (some APID).
C021	2024-09-25 13:47:54	2024-09-25 14:52:56	Passes 422 to 423 : 91.13 % and 28.93 % of missing data over ocean.
C021	2024-09-30 12:06:12	2024-09-30 13:07:46	Passes 560 to 561 : 93.49 % and 32.03 % of missing data over ocean to data loss.
C022	2024-10-02 18:55:18	2024-10-02 20:23:53	Passes 040 to 041 : 80.05% and 93.86% over ocean.
C022	2024-10-03 03:00:58	2024-10-03 03:34:57	Passes 049 to 050 : 13.60% and 14.22% over ocean due to data loss.
C022	2024-10-06 15:42:07	2024-10-06 17:26:32	Passes 148 to 150 : 81.46%, 100% and 13.60% over ocean due to data loss.
C022	2024-10-07 16:59:30	2024-10-07 18:43:22	Passes 177 to 179 : 5.73%, 100.00% and 94.68% over ocean due to downlink passes conflict.
C022	2024-10-08 00:04:33	2024-10-08 00:27:21	Pass 186 : 41.98% over ocean due to data loss.
C022	2024-10-11 13:16:24	2024-10-11 14:37:27	Passes 285 to 287 : 43.28%, 100% and 8.70% over ocean due to OCM SLOT maneuver.
C022	2024-10-14 11:46:19	2024-10-14 11:46:38	Pass 367 : 1.13% over ocean (less than one minute).
C022	2024-10-15 17:28:33	2024-10-15 19:17:19	Passes 402 to 404 : 66.21%, 100% and 25.86% over ocean due to data loss.
C022	2024-10-20 13:12:17	2024-10-20 13:24:28	Pass 537 : 31.03% over ocean due to data loss.
C023	2024-10-24 09:43:37	2024-10-24 10:33:26	Passes 061 and 062 : 78.62% and 13.76% over ocean due to corrupted data.
C023	2024-10-25 22:33:02	2024-10-25 22:33:02	Passes 104 and 105 : 79.11% and 79.06% over ocean due to downlink not received.
C023	2024-10-30 08:10:15	2024-10-30 08:35:41	Pass 227 : 17.66% over ocean due to downlink cancelled.

Cycle	Start	End	Details
C023	2024-10-30 19:05:16	2024-10-30 22:21:24	Passes 240 to 243 : 94.17%, 100%, 58.70% and 87.61% over ocean due to antenna issue resulting to downlink cancelled.
C023	2024-11-01 10:44:01	2024-11-01 12:14:36	Passes 286 to 288 : 87.04 %, 100.00 % and 11.48 % over ocean to an antenna issue resulting in data loss.
C023	2024-11-01 17:37:24	2024-11-01 17:39:02	Pass 294 : 0.74% over ocean due to data gaps.
C023	2024-11-01 19:02:26	2024-11-01 19:06:57	Pass 296 : 2.55% over ocean due to data gaps.
C023	2024-11-01 20:48:12	2024-11-01 20:51:48	Pass 298 : 2.34% over ocean due to data gaps.

Table 7: List of missing GDR SWOT Nadir passes from C001 to C023

3.6. Edited measurements

Editing criteria allow to select only measurements considered as valid over ocean. This editing process is structured in 3 main steps:

1. Latitude monotony is checked;
2. Measurements over land are removed, only measurements over ocean are kept;
3. Measurements over ice are removed;
4. Threshold criteria are applied on altimeter, radiometer and geophysical parameters as described in the following table 8. This step includes the rejection of measurements at Default Value (DV).

3.6.1. Maneuvers

Maneuvers impact either availability or validity, or both. The following editing statistics include maneuver zones for which data is available.
Note that for the folllowing figures, the peaks of edited measurements correspond to maneuvers that took place during the study period and listed in table 2. Maneuvers will be highlighted by the colored vertical lines on the editing figures to follow. Each color corresponds to a specific maneuver as highlighted in Table1. Figure 19 (left) displays the days on which a maneuver occured as the count per day of measurements taken during a maneuver. A count of 0 means there was not any maneuver on this day. The map (Fig. 19, right) shows the spatial distribution of measurements concerned by maneuvers over ocean.

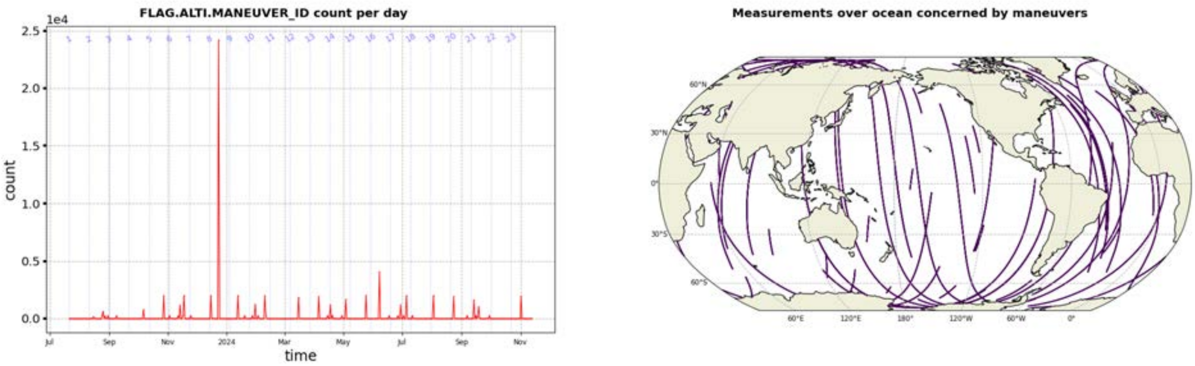

Figure 19: Points concerned by maneuvers over C001 to C023 period

3.6.2. Editing

The percentage of total edited measurements over ocean is monitored on a cyclic basis. The average of total valid measurements over ocean is 82.54% (see Figure 20).
EEPROM update on 12 Sep. 2023 (C003) has a slight impact on edited data because more data near ice lands are available (see figure 17).

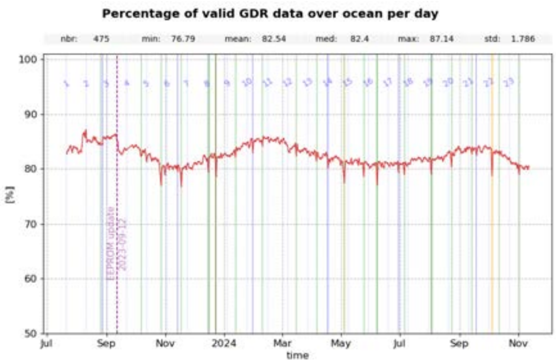

Figure 20: SWOT Nadir ocean data editing average by day.

3.6.3. Flagging quality : ice

The GDR ice flag (from L2 variable *ice_flag*) is used to remove the ice and sea ice data. Figure 21 shows daily percentage of measurements edited by this criterion over ocean. Over the 23 cycles, in average 14.79% of data were edited by this criterion over ocean. Over the shown period, no anomalous trend is detected, only the annual seasonal signal is visible mainly due to ice coverage annual variations in north and south hemispheres.

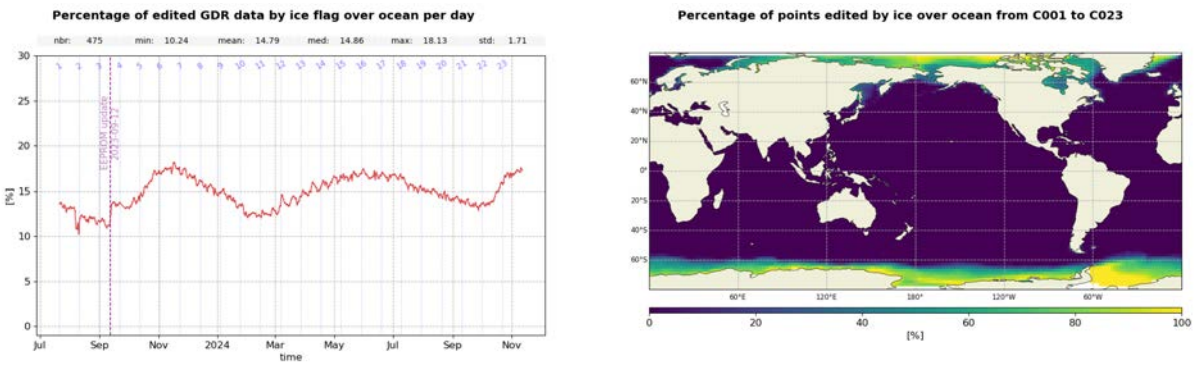

Figure 21: Cyclic monitoring of the percentage of edited measurements by ice flag criterion over ocean

3.6.4. Thresholds

3.6.4.1. Overview

After quality flag analysis, instrumental parameters have also been analyzed from comparison with thresholds. The average of total edited measurements following threshold criterion is around 2.76% (Figure 22). For each criterion, daily percentage of edited measurements is monitored (detailed later). This allows the detection of anomalies in the number of removed data, which could be of instrumental, geophysical or algorithmic origins. Note that all outliers are on maneuver slots (colored lines).

Threshold criteria applied on altimeter, radiometer and geophysical parameters are described in the following table 8. The last column represents the mean of rejected data on each criterion over GDR cycles 001 to 023.

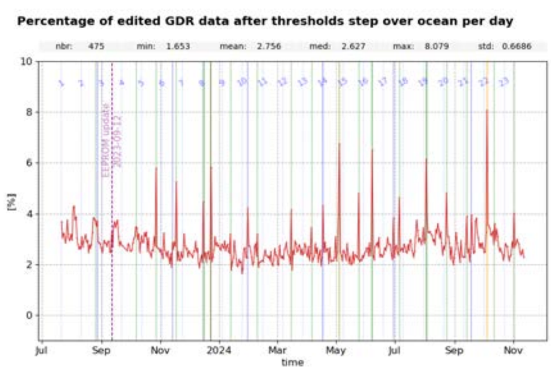

Figure 22: SWOT Nadir data editing by thresholds over ocean average by day.

Parameters	**Min threshold**	**Max threshold**	**Unit**	% **rejected** (DV included)
Sea surface height anomaly	-2	2	m	1.69
Sea surface height	-130	100	m	0.46
Nb measurements of range	10	20		0.58
Std. deviation of range	0	0.2	m	1.10
Backscatter coefficient	7	30	dB	0.41
Nb measurements of sigma0	10	20		0.58
STD of sigma0	0	1	dB	1.22
Significant wave height	0	11	m	0.43
Altimeter wind speed	0	30	$m.s^{-1}$	0.73
Sea State Bias	-0.5	0	m	0.35
Filtered ionospheric correction	-0.4	0.04	m	0.82
Square off nadir angle	-0.2	0.64	deg^2	0.40
Equilibrium tide	-0.5	0.5	m	0.00
Inverted barometer correction	-2	2	m	0.00
Dry tropospheric correction	-2.5	-1.9	m	0.00
Internal tide	-5	5	m	0.00
Ocean tide	-5	5	m	0.002
Pole tide	-15	15	m	0.00
Earth tide	-1	1	m	0.00
Wet Tropospheric Correction (WTC)	-0.5	-0.001	m	0.11
Global statistics of edited measurements by thresholds				**2.76**

Table 8: Table of parameters used for editing and the corresponding percentages of edited measurements for each parameter for SWOT Nadir GDR for cycle 001 to 023.

3.6.4.2. Individual thresholds: 20Hz range measurement number and standard deviation

1Hz range measurements computed with less than 10 elementary measurements (range_number < 10) are rejected. These are considered as not consistent to compute 1Hz resolution range. Waveforms are distorted by rain cells, which makes them often meaningless for SSH calculation. As a consequence, edited measurements due to several altimetric criteria are often correlated with wet areas.
The average percentage of removed measurements using this criterion is 0.58% (Figure 23, left). Some parts of passes are edited over ocean because of undefined retracking outputs or/and radiometer wet tropospheric correction due to maneuvers that directly impact data. They correspond to the part of passes in figure 24 and to the peaks visible in figure 23.
Using the threshold editing on 20Hz measurements standard deviation (Figure 23, right), 1.10% of data are removed in average. As for 20Hz range number & std criterion, edited measurements are correlated with wet areas (Figure 24).

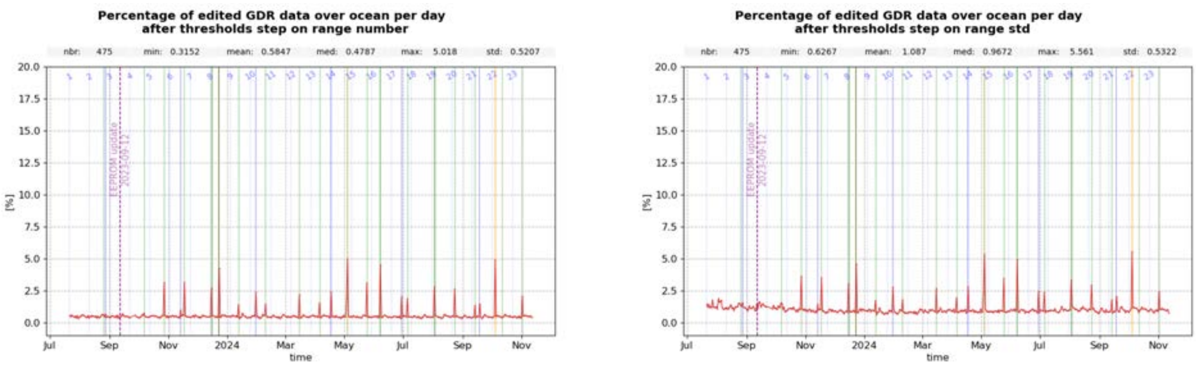

Figure 23: Percentage of edited measurements by 20Hz range measurement threshold criterion.

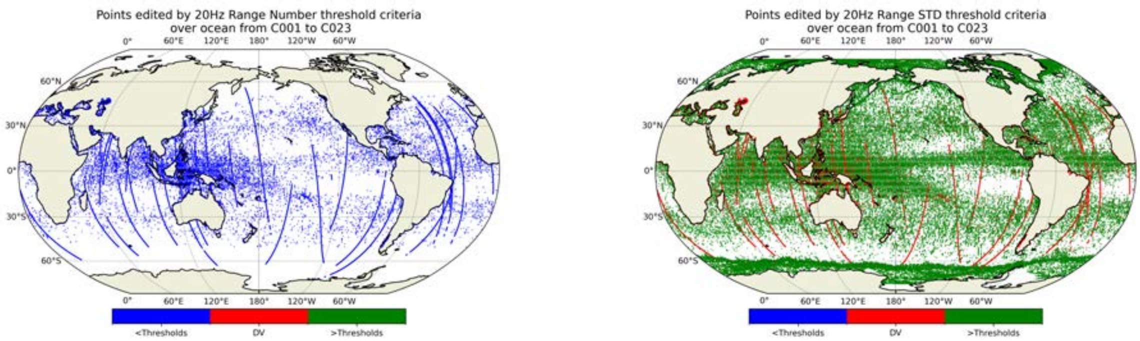

Figure 24: Map of edited measurements by 20Hz range measurements threshold criterion

3.6.4.3. Individual thresholds: Significant Wave Height (SWH)

The percentage of edited measurements due to significant wave heights criterion is represented on Figure 25, and is about 0.43%. The peaks visible in figure 25 left correspond to the portions of passes at DV visible in figure 25 right, they are related to maneuvers as explained in section 3.6.4.2..

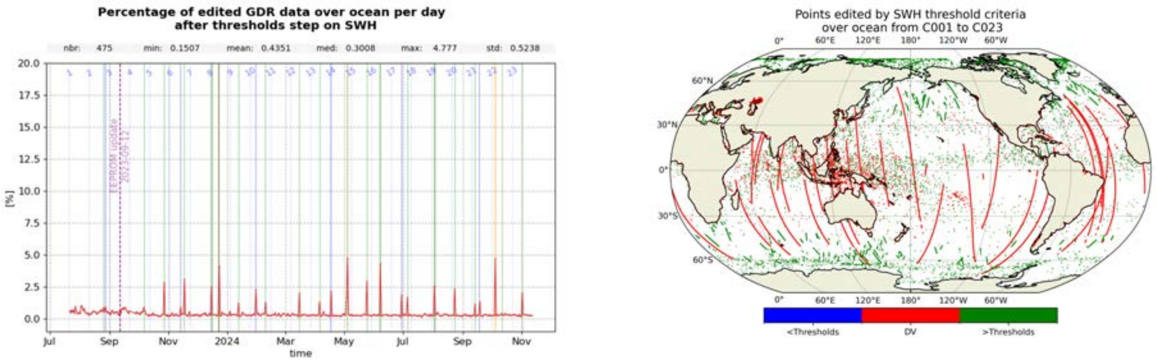

Figure 25: Edited measurements by SWH threshold criterion.

3.6.4.4. Individual thresholds: Backscatter coefficient (Sigma0)

The percentage of edited measurements due to backscatter coefficient criterion is represented on Figure 26. Peaks and part of passes rejected are related to maneuvers as explained in section 3.6.4.2..

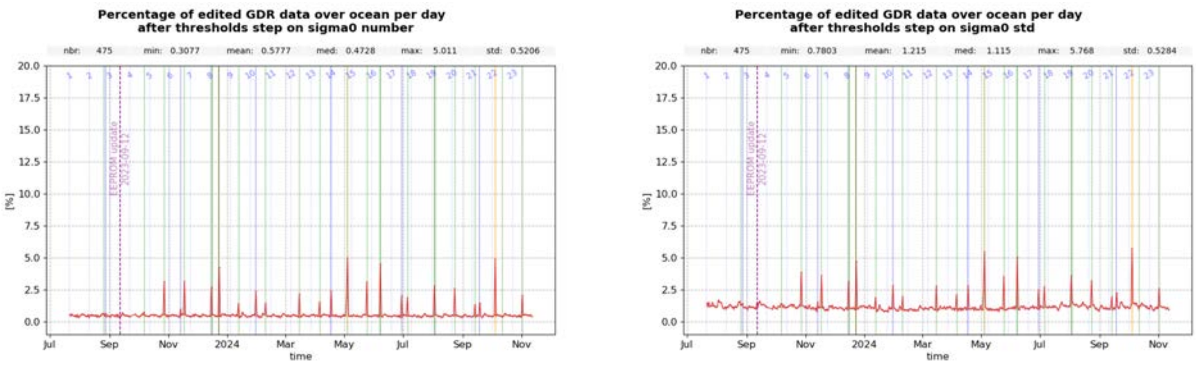

Figure 26: Percentage of edited measurements by 20Hz backscatter coefficient threshold criterion.

3.6.4.5. Individual thresholds : Altimeter wind speed

The percentage of edited measurements due to altimeter wind speed criterion is represented on figure 28. Measurements are usually edited because of default values (section 3.6.4.4.). This is the case when sigma0 itself is at default value (as seen in section 3.6.4.4.), or when it shows very high values (higher than 25 dB), which occurs during sigma bloom situations and also over sea ice. Indeed, the wind speed algorithm (which uses backscatter coefficient and significant wave height) can not retrieve values for sigma0 higher than 25 dB.

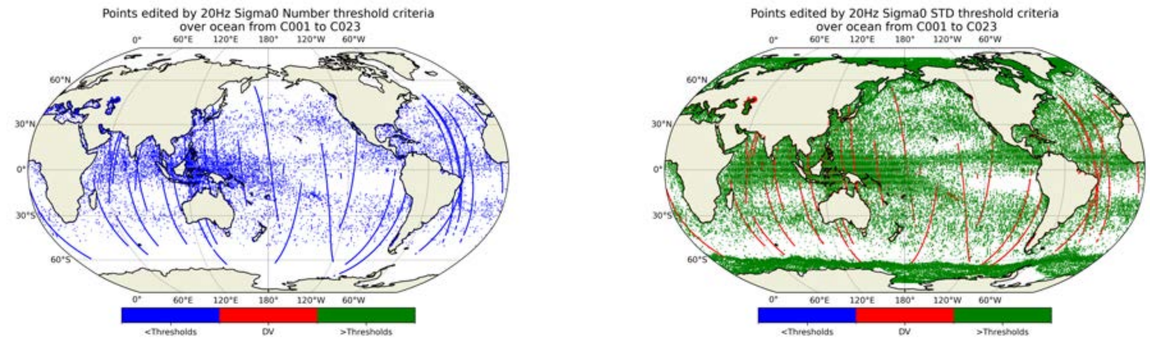

Figure 27: Map of edited measurements by 20Hz backscatter coefficient threshold criterion

Caution: there are negative altimeter wind speed values in the product but in our internal validation database negative values are set to DV.
Nevertheless, sea state bias is available even for negative wind speed values. Therefore, the percentage of edited altimeter wind speed data is higher than the percentage of edited sea state bias data (see part 3.6.4.6.).
The figure 28 showing percentage of measurements edited by altimeter wind speed criterion is correlated with figures 25 (SWH) and 29 (SSB).

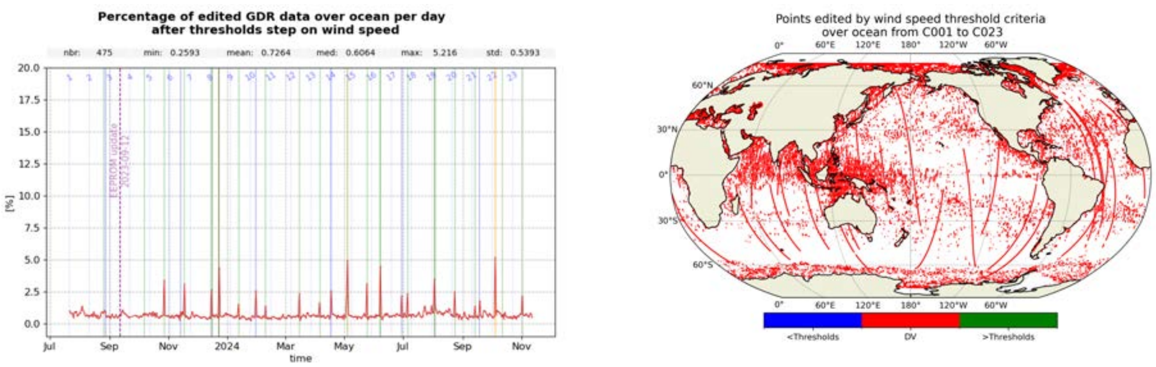

Figure 28: Edited measurements by wind speed threshold criterion.

3.6.4.6. Individual thresholds : Sea State Bias (SSB)

Regarding the sea state bias criterion, the percentage of SWOT Nadir edited measurements is about 0.35%. The difference can also be observed on the sigma0 and the significant wave height threshold criteria (which are both used for SSB computation).

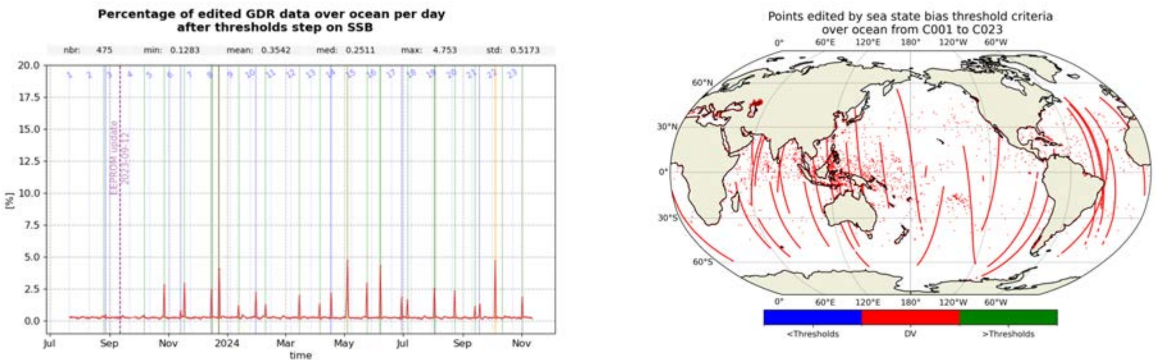

Figure 29: Edited measurements by sea state bias threshold criterion.

3.6.4.7. Individual thresholds : Ionospheric correction

The mean percentage of edited data by threshold criterion on filtered ionospheric correction is 0.82%. As ionospheric correction is computed as a combination from Range and SSB (ku and c bands), peaks and DV sections are visible. Due to filtering, small areas of rejected SSB and Range measurements are filled (this explains why we do not see these areas appear yet rejected on the other maps).

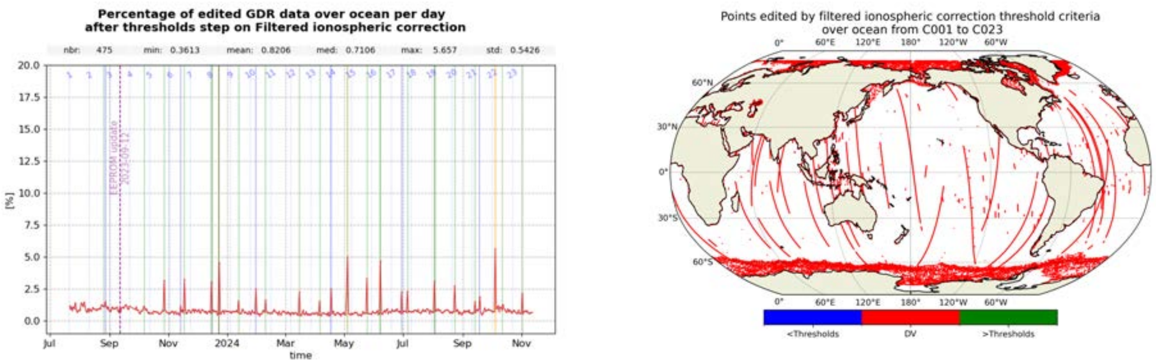

Figure 30: Edited measurements by ionospheric correction threshold criterion.

3.6.4.8. Individual thresholds: Radiometer wet troposphere correction

The percentage of edited measurements due to radiometer wet troposphere correction criterion is represented in figure 31. As for retracking outputs, during maneuvers geolocation problems make interpolation of the 2 radiometers impossible and therefore values are at DV.

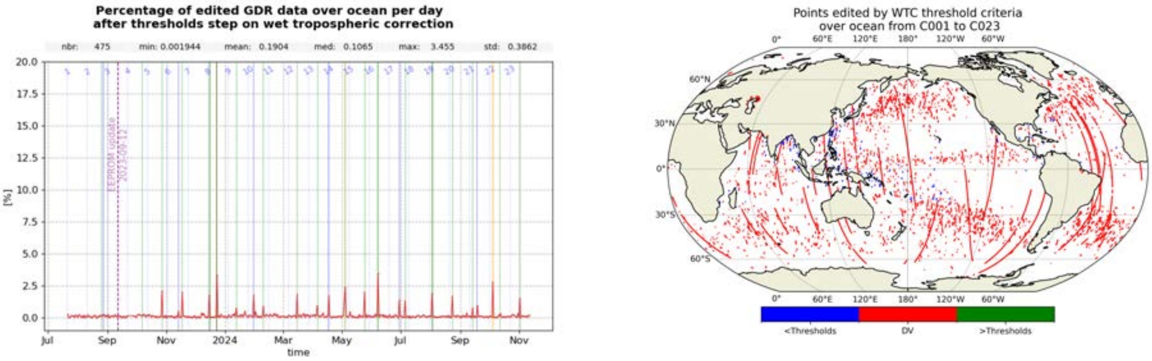

Figure 31: Edited measurements by radiometer wet troposphere correction threshold criterion.

3.6.4.9. Individual thresholds : Ocean tide

The percentage of edited measurements due to ocean tide is lower than 0.002%. The ocean tide correction is a model output, there should therefore be no edited measurement, the few edited points are linked to the coast interpolation.

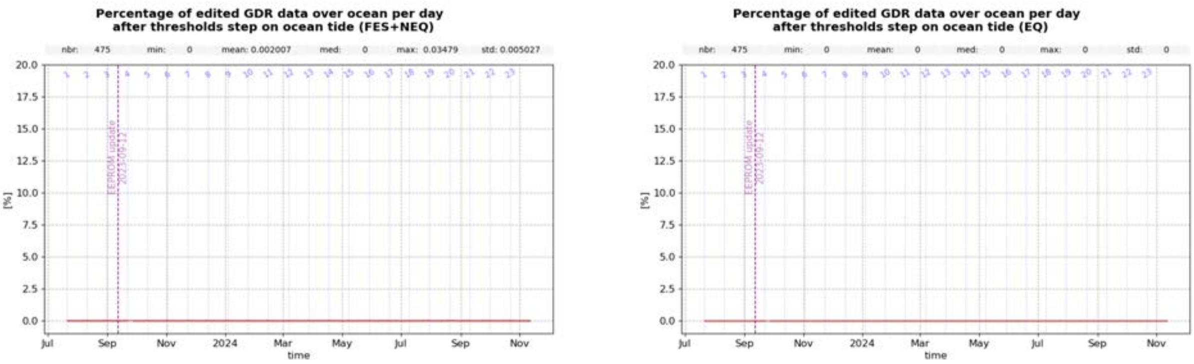

Figure 32: Percentage of edited measurements by ocean tide and ocean tide equilibrium threshold criterions.

3.6.4.10. Individual thresholds : Square off nadir angle

The percentage of edited measurements due to mispointing is about 0.39%. Peaks and part of passes rejected are related to maneuvers as explained in section 3.6.4.2..

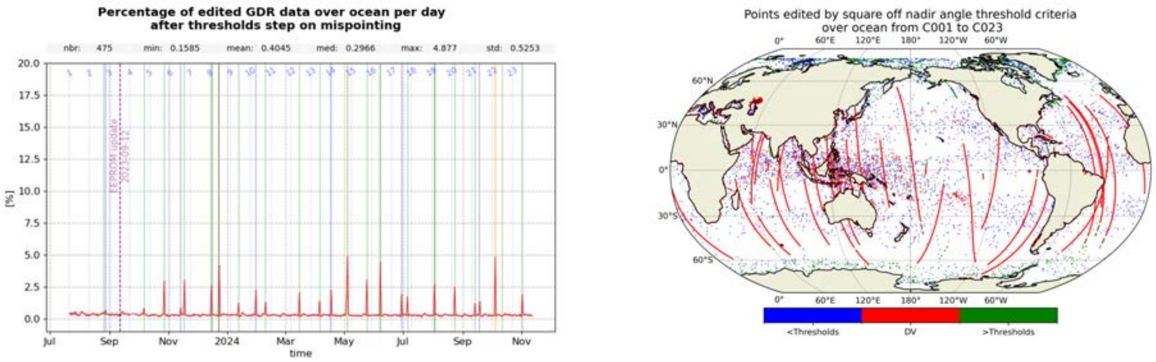

Figure 33: Edited measurements by square off nadir angle threshold criterion.

3.6.4.11. Individual thresholds : SSH

Sea surface height represents the difference between the orbit and the altimeter range.
Figure 34 summarizes the editing resulting from the sea surface height threshold criterion. It removes in average 0.46% of data for SWOT Nadir. The editing is usually due to range measurements at default values near coast in equatorial and mid-latitude regions, as well as regions with low significant wave heights. Moreover, peaks and part of passes rejected are related to maneuvers as explained in section 3.6.4.2..

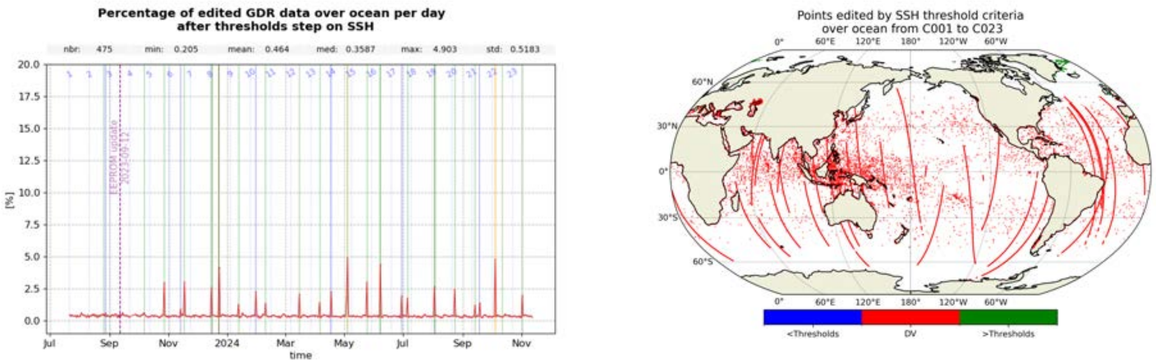

Figure 34: Edited measurements by sea surface height threshold criterion.

3.6.4.12. Individual thresholds : SLA

The percentage of edited data by threshold criterion on SLA is 1.69%. Peaks and part of passes rejected are related to maneuvers as explained in section 3.6.4.2..

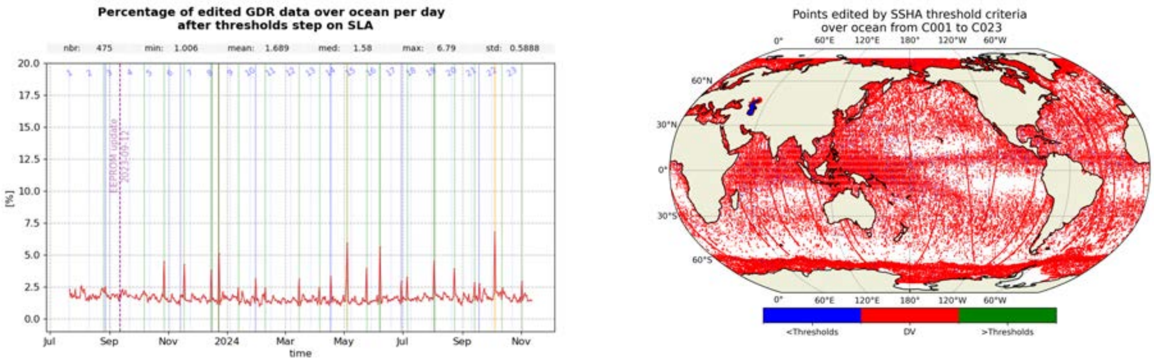

Figure 35: Edited measurements by sea level anomaly threshold criterion.

4 Monitoring of altimeter and radiometer parameters

Note that from this section, we only monitor statistics on valid measurements. Mean and standard deviation of SWOT Nadir main parameters have both been monitored in this report since the beginning of the Science Phase.

4.1. 20Hz measurements

The monitoring of the number and standard deviation of 20 Hz elementary range and backscatter coefficient measurements used to derive 1 Hz data is presented here. These two parameters are computed during the altimeter ground processing. As for Jason-3, Jason-2 and Sentinel-6A-MF, before performing a regression to derive the 1 Hz measurements from 20 Hz data, a MQE (mean quadratic error) criterion is used to select valid 20 Hz measurements. This first step of selection consists in verifying that the 20 Hz waveforms can be approximated by a Brown echo model (Brown, 1977 [15], Thibaut et al. 2002 [16]). Then, through an iterative regression process, elementary measurements too far from the regression line are discarded until convergence is reached. Thus, monitoring the number of 20 Hz measurements and the standard deviation computed among them is likely to reveal changes at instrumental level. The change in Altimeter characterization file visible on figures 36 and 37 left has aligned mean values of IGDR and GDR. Standard deviation of range measurements is correlated with significant wave height (SWH dedicated part: 4.3.).

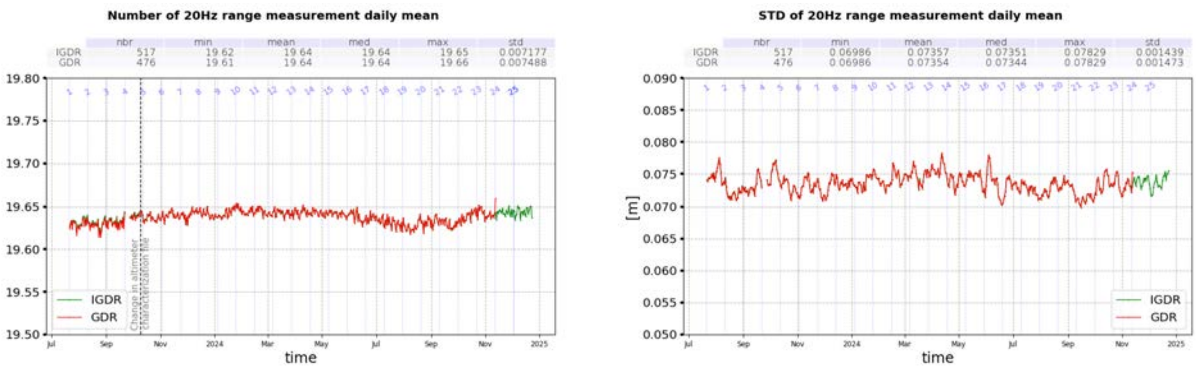

Figure 36: Daily monitoring of elementary 20 Hz range measurements

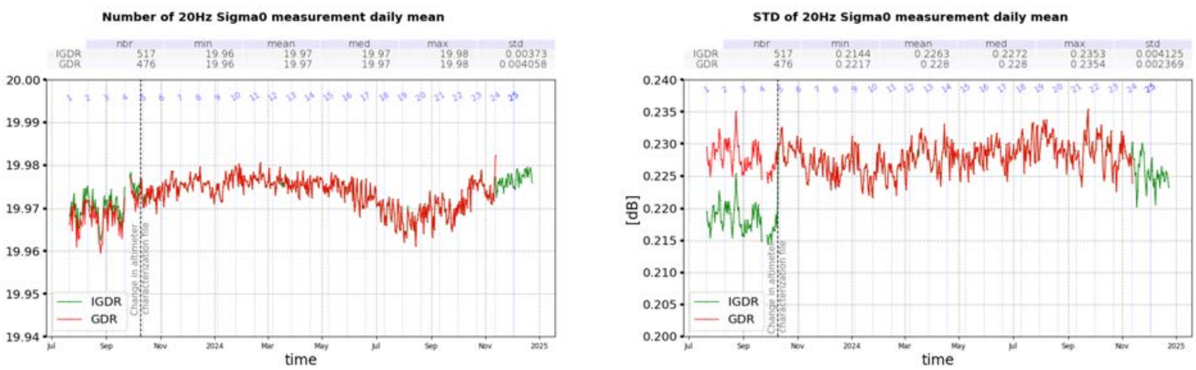

Figure 37: Daily monitoring of elementary 20 Hz sigma0 measurements

4.2. Off-nadir angle from waveform

The off-nadir angle is derived from the slope of the trailing edge of the waveform during the altimeter processing : it can either be caused by real platform mispointing or by backscattering properties of the surface.
The square of the off-nadir angle, averaged on a daily basis (taking into account valid measurements only), has been plotted on figure 38.
The significant jump for IGDR on both mean and std of square off nadir angle is explained by an update of the characterization file of the altimeter applied to IGDR from 2023-10-09 23:24:06 (Cycle 4 Pass 509). GDR were homogeneously processed with the last version of the characterization file.
The low amplitude periodic signal in mean value of mispointing is linked to platform mispointing coming from spacecraft attitude variation (Fig. 38, left). On the other side, the period of the signal for std seems to depict an annual variability linked to the coverage variability (Fig. 38, right). Despite this periodic signal, mispointing values for SWOT Nadir are quite stable in time. Nevertheless, there are two small periods where mispointing is higher than usual but still within thresholds: on 2024-05-04, for cycle 14 during gyro calibrations period (from 12:20:02 to 21:43:01) and also on 2024-10-04 (cycle 22) due to gyro calibrations (from 10:25:57 to 19:28:56).

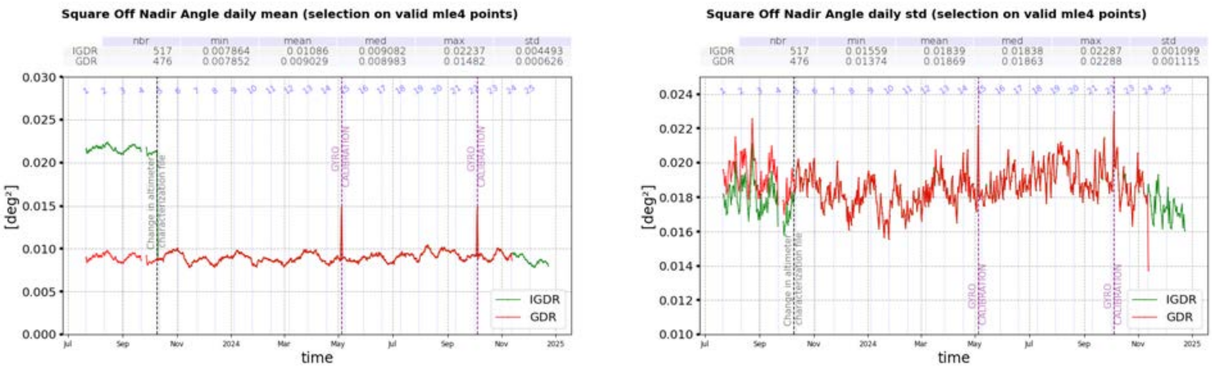

Figure 38: Daily monitoring of the square off-nadir angle.

4.3. Significant wave height

Ku-band wave estimations derived from altimeter measurements are monitored in this section.
SWOT Nadir SWH is centered around 2.57 m for MLE4 (figure 39, top left). Comparison to ERA5 model shows a jump around cycle 10 that affects GDR and IGDR, it is linked to the introduction of Cryosat-2 (C2N) in ERA5 model and it is also visible in other mission as Sentinel-6A-MF. The mean of differences tends to be higher after cycle 10 (figure 39, bottom left) while the standard deviation tends to be slightly reduced.

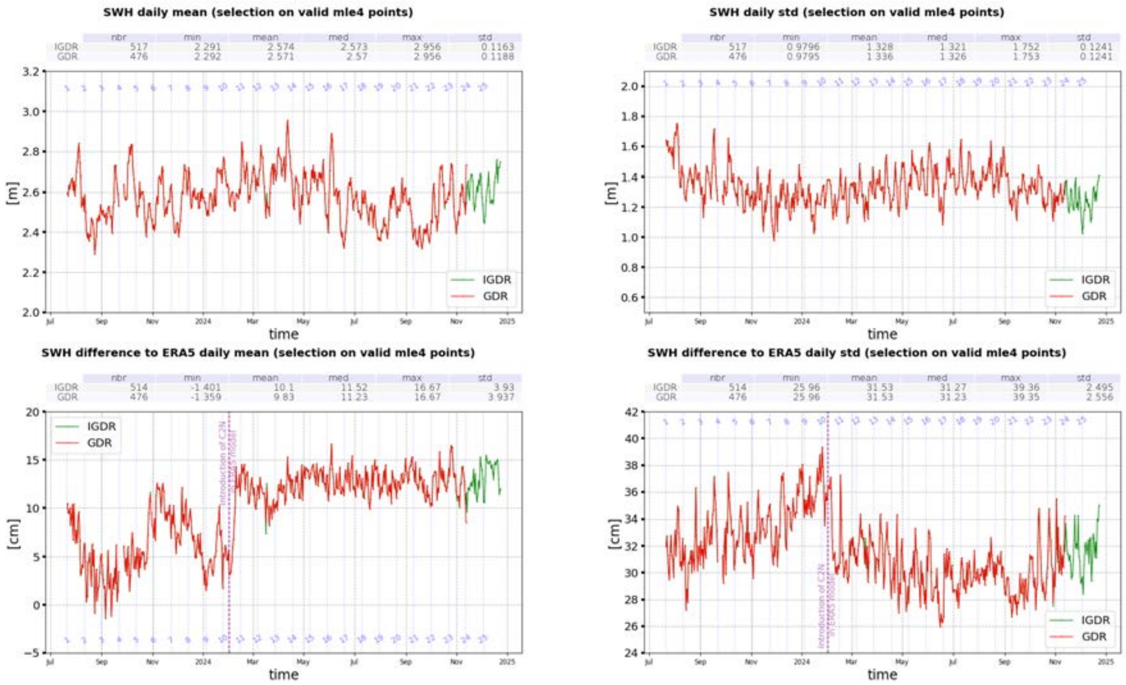

Figure 39: Monitoring of significant wave height

Figure 40 shows the maps of the mean difference between altimeter and ERA5 model SWH for a winter cycle (cycle 11, left) and a summer cycle (cycle 18, right).

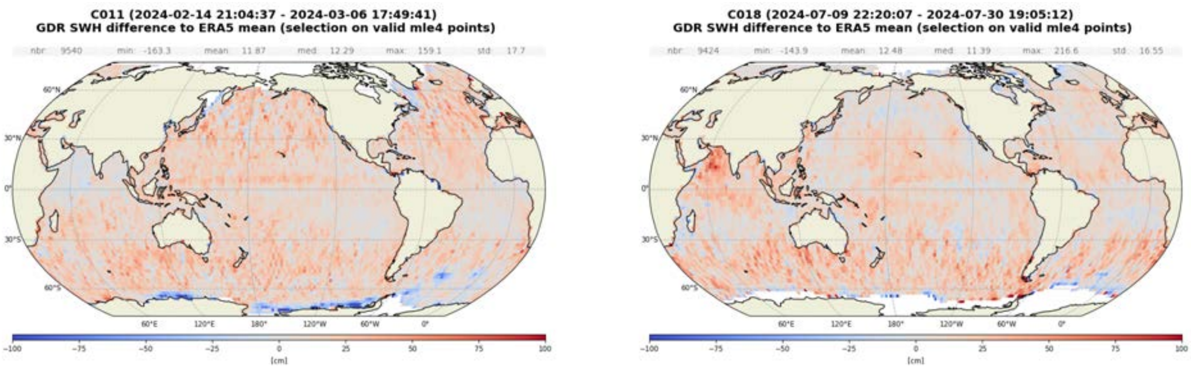

Figure 40: Cyclic monitoring of swh difference to ERA5 model

4.4. Backscatter coefficient

SWOT Nadir Ku-band backscatter coefficient is stable around 13.47dB for the period (figure 41).
The slight decrease for IGDR on mean of sigma0 is explained by an update of the characterization file of the altimeter applied to IGDR from 2023-10-09 23:24:06 (Cycle 4 Pass 509).

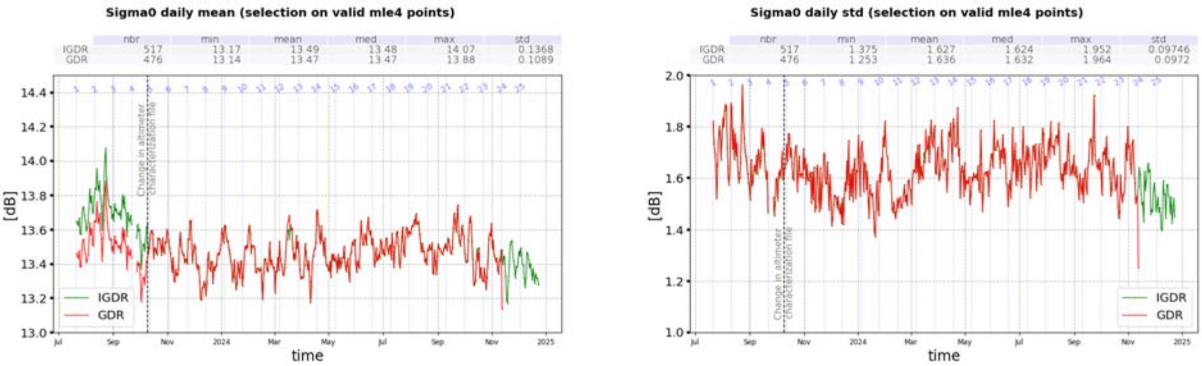

Figure 41: Daily monitoring of sigma0 measurements

4.5. Wind speed

Altimeter wind speed is derived from backscattering coefficient and significant wave height using Collard algorithm. To allow wind speed computation, a calibration bias is applied on the backscattering coefficient. For the current version of GDR, wind speed are not fitted to SWOT Nadir data, but the same biases as for Jason-3 GDR-F are applied. As a consequence, wind speed estimations are not aligned with ERA5 model in the GDR-F v1.04 version (figure 43).
The increase for IGDR of altimeter wind speed is explained by an update of the characterization file of the altimeter applied to IGDR from 2023-10-09 23:24:06 (Cycle 4 Pass 509). The daily average from cycle 001 to cycle 023 shows the wind speed values centered around 8.51 m/s for MLE4 (figure 42).

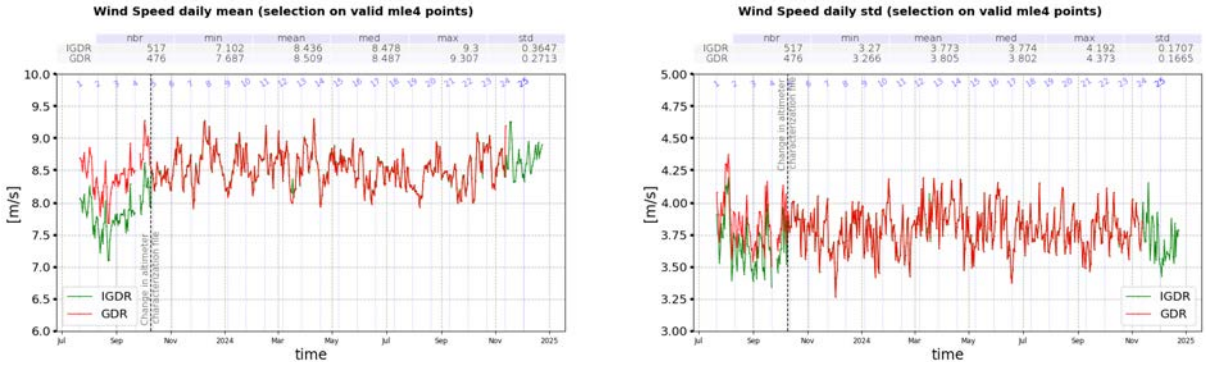

Figure 42: Monitoring of altimeter wind speed

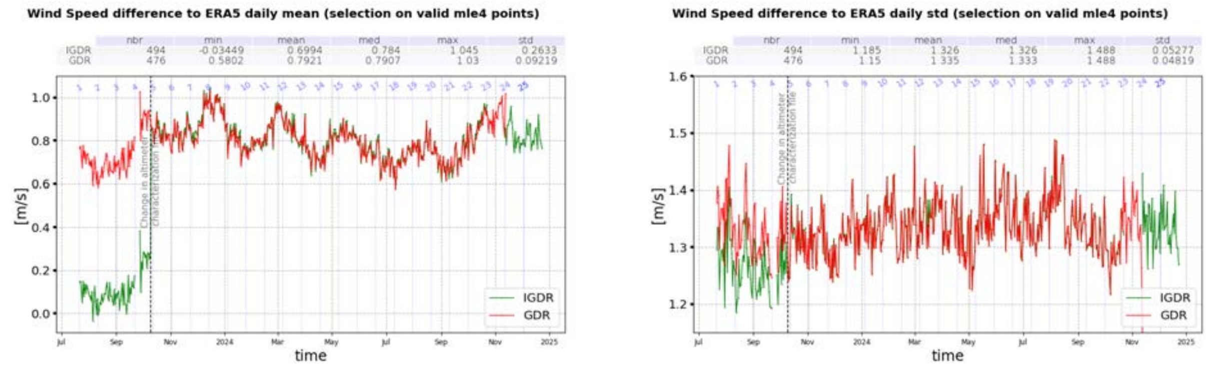

Figure 43: Monitoring of altimeter wind speed difference to ERA5 model

Figure 44 shows the maps of the mean difference between altimeter and ERA5 model Wind Speed for a winter cycle (cycle 11, left) and a summer cycle (cycle 18, right).

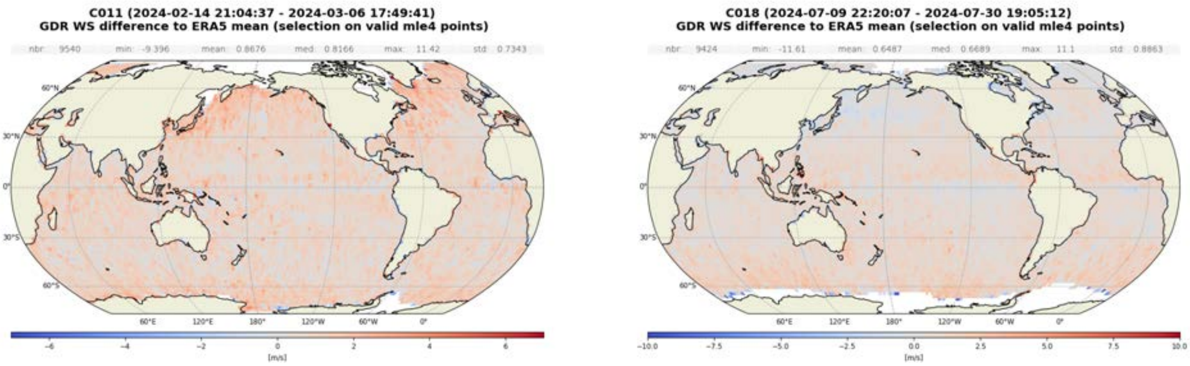

Figure 44: Cyclic monitoring of wind speed difference to ERA5 model

4.6. Sea state bias

For the current version of GDR, SSB is not fitted to SWOT Nadir data, but the same biases as for Jason-3 GDR-F are applied. SWOT Nadir sea state bias is centered around -10.13 cm for MLE4 (figure 45).

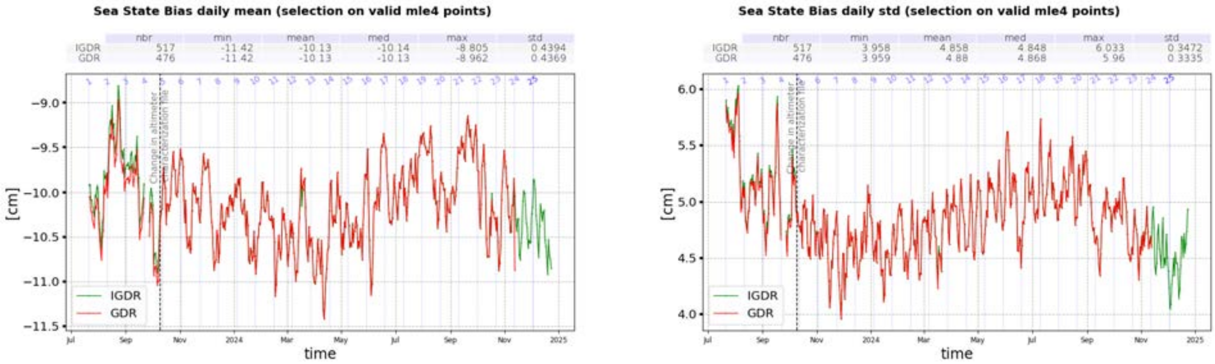

Figure 45: Monitoring of sea state bias

4.7. Ionospheric correction

SWOT Nadir altimeter filtered ionospheric correction is centered around -6.30 cm for MLE4 retrievals (figure 46). We are curently in an increasing phase of solar activity and there was several solar storm in 2024, thus it impacts directly the ionospheric correction.
There were anomalies in tec/gim files in March from 5th to 7th and in May from 26th to 29th impacting the difference between instrumental and model (GIM) ionospheric corrections, they are visible with the 2 jumps at the end of cycle 11 and cycle 15 respectively (purple lines, figure 47).

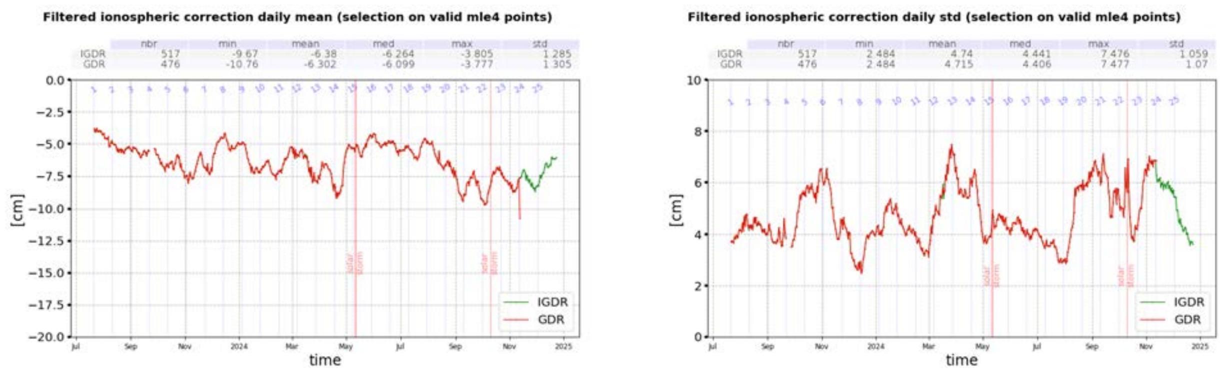

Figure 46: Monitoring of filtered ionospheric correction

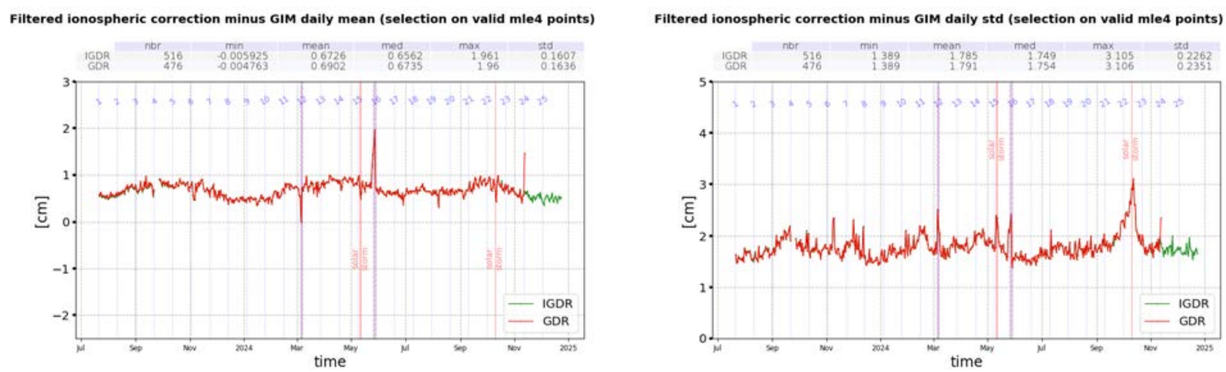

Figure 47: Monitoring of filtered ionospheric correction difference to GIM model

Note that an iterative filtering method was applied to the ionospheric correction in the production of SWOT Nadir GDR-F altimetry products. The process is applied to the non filtered solution computed from the formula:

$$Iono = \delta f\,[(Range_{Ku} + SSB_{Ku}) - (Range_C + SSB_C)]$$

where $\delta f = \dfrac{(FrequencyC_{band})^2}{(FrequencyKu_{band})^2 - (FrequencyC_{band})^2}$ represents the frequency factor

For SWOT Nadir, frequency is 5.3GHz for C-band and 13.575GHz kor Ku-band.
The iterative filtering scheme was developed to achieve two main goals:

- Base the correction on as many dual-band ionospheric observations as possible
- Improve the correction where altimetric observations are discontinuous or isolated.

This method is fully detailled from Nencioli *et al.* [13] in Jason-3 GDR-F Reprocessing bilan [14].

As ionospheric correction is strongly linked to day/night time measurements, the 3 examples of the local hours distribution and their corresponding ionospheric correction are displayed below (Fig. 48, 49 and 50). For cycle 013 ascending passes are measuring over equator by day but by night for descending passes (Scenario A, Fig. 48). For cycle 016, it’s the opposite of what is done for cycle 013 with ascending equatorial measurements by night and by day for descending (Scenario C, Fig. 50). And cycle 014 presents an intermediate configuration between cycles 013 and 016 (Scenario B).

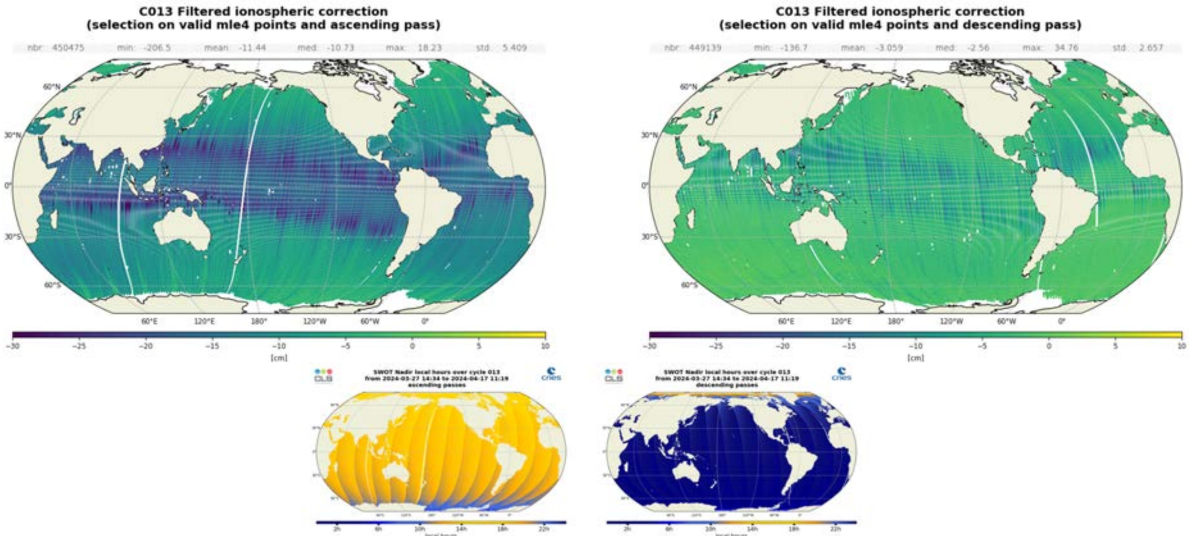

Figure 48: Ionospheric correction distribution for ascending and descending passes [Scenario A]

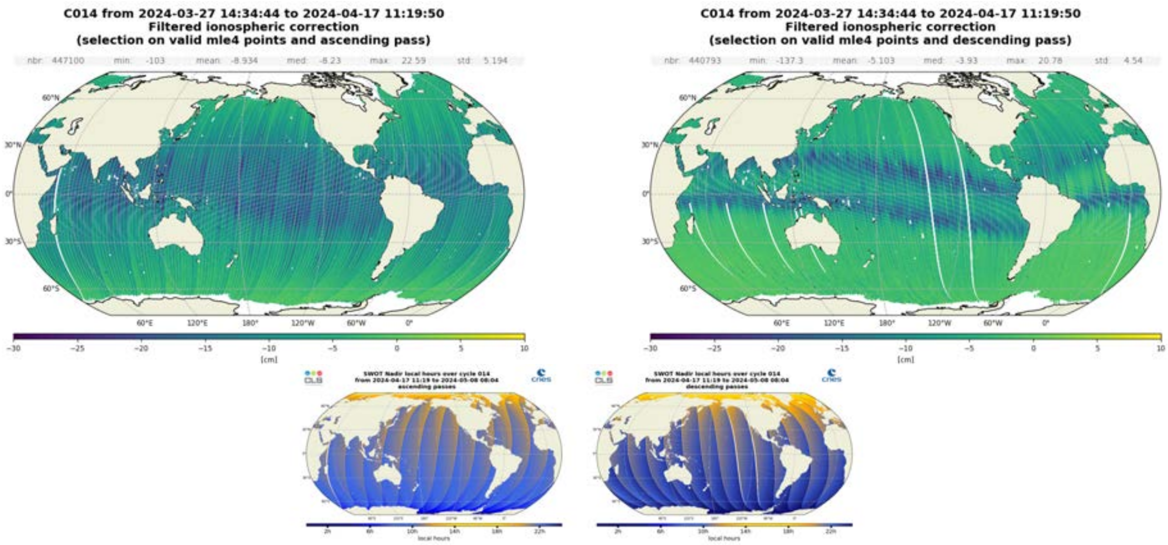

Figure 49: Ionospheric correction distribution for ascending and descending passes [Scenario B]

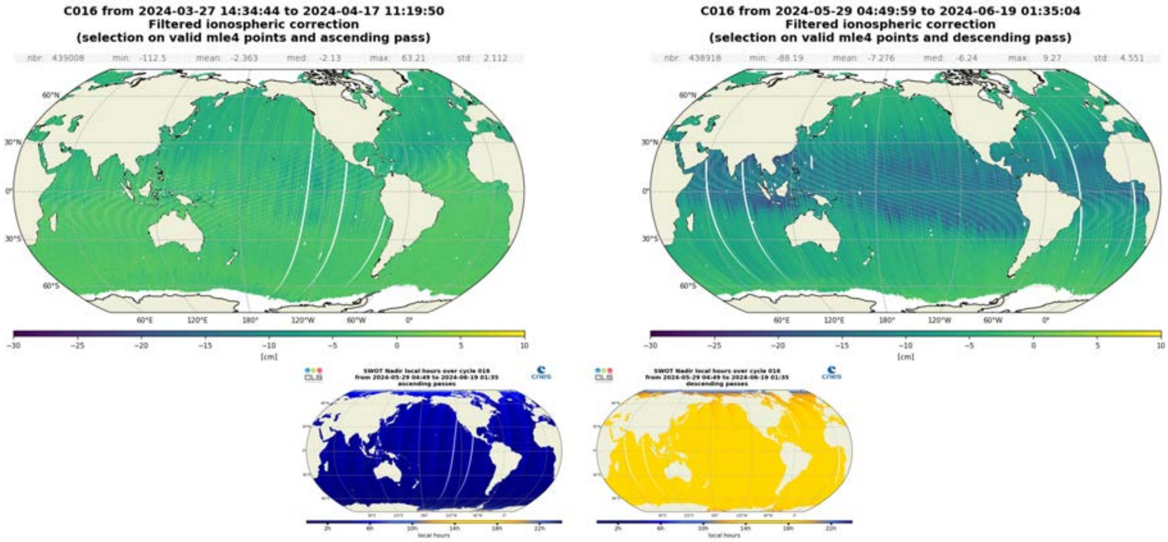

Figure 50: Ionospheric correction distribution for ascending and descending passes [Scenario C]

5 Validation and Monitoring of Radiometer Parameters

5.1. Geophysical products monitoring

For the SWOT mission, the Wet Tropospheric Correction is measured by a radiometer with two independants beams, measuring tropospheric correction on each side of the nadir, with AMR Side 1 35 km away from nadir, and Side 2 40 km away. Depending of Yaw Flip, one beam measure the Wet Tropospheric Correction slightly fore of the Nadir Altimeter measurement, while the other beam measure aft of Nadir Altimeter measurement. Then, an interpolation using the two radiometer sides is performed to obtain the Wet Tropospheric Correction on each 1Hz altimeter measurement.

Figure 51 shows the daily monitoring of the Nadir Wet Tropospheric Correction for both IGDR and GDR, for every valid MLE4 points, with a mean value around -16cm and a standard deviation around 10.15 cm.

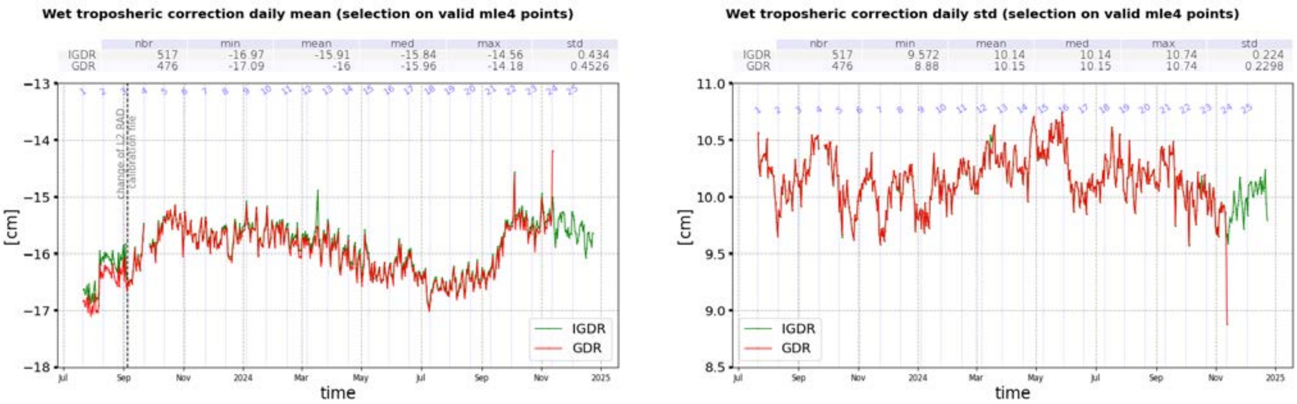

Figure 51: Daily monitoring of the Wet Tropospheric Correction for IGDR (green) and GDR (red), from Cycle 1 to Cycle 23

Figure 52 shows the evolution of the Wet Tropospheric Correction measured by both radiometer beams and interpolated on the Nadir for every Nadir points where the interpolated WTC is considered as valid, and closest S1 and S2 L2RAD points are valids too, to have the same selection for all datasets. The variations observed are mainly due to seasonal effects and geophysical events as El Nino.

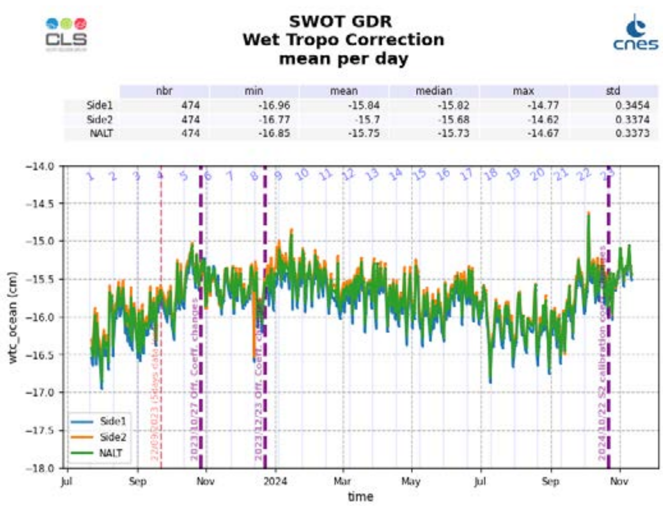

Figure 52: Daily monitoring of the mean of the Wet Tropospheric Correction for the AMR S1 (blue), AMR S2 (orange) and Nadir (green) from Cycle 1 to Cycle 23

To assert the quality of the WTC from the satellite, it is compared to a WTC computed from the ECMWF operational model, available every 6 hours. This model WTC is then linearly interpolated at both radiometer beams measurements locations and Nadir locations. Figure 53 shows the daily monitoring of the difference between Nadir WTC and model WTC for both IGDR and GDR. This indicator is stable around 0.32 cm, with a standard deviation of 0.96cm. The IGDR-only peak at the beginning of cycle 5 is due to a location problem in radiometer products which impacts the nadir interpolation, which was corrected in GDR.

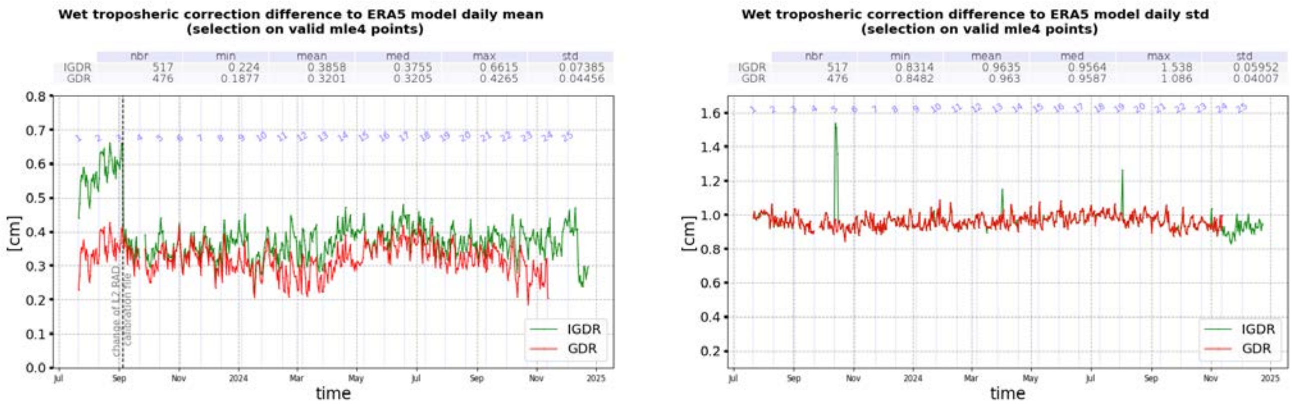

Figure 53: Daily monitoring of the difference between WTC interpolated at Nadir and WTC from model for IGDR (green) and GDR (red), from Cycle 1 to Cycle 23

Figure 54 shows the evolution of the daily mean and standard deviation of the difference between both AMR beams WTC and Nadir WTC, and model WTC, for every Nadir points where the interpolated WTC is considered as valid, and closest S1 and S2 L2RAD points are valids too, to have the same selection for all datasets. This shows the stability of SWOT's WTC with variation of mean of no more than one mm apart from calibration changes. After 2023-10-21 change in radiometer calibration coefficients, the mean difference for both radiometer's sides and Nadir appears is almost identical, around 0.3 cm/ The daily standard deviation is stable too, around 1.1 cm for the radiometer, which is the nominal standard deviation expected (similar to Jason-3 and Sentinel-6).The daily standard deviation of the difference is only 0.9 cm for the Nadir interpolated WTC, due to the smoothing effect of the interpolation.

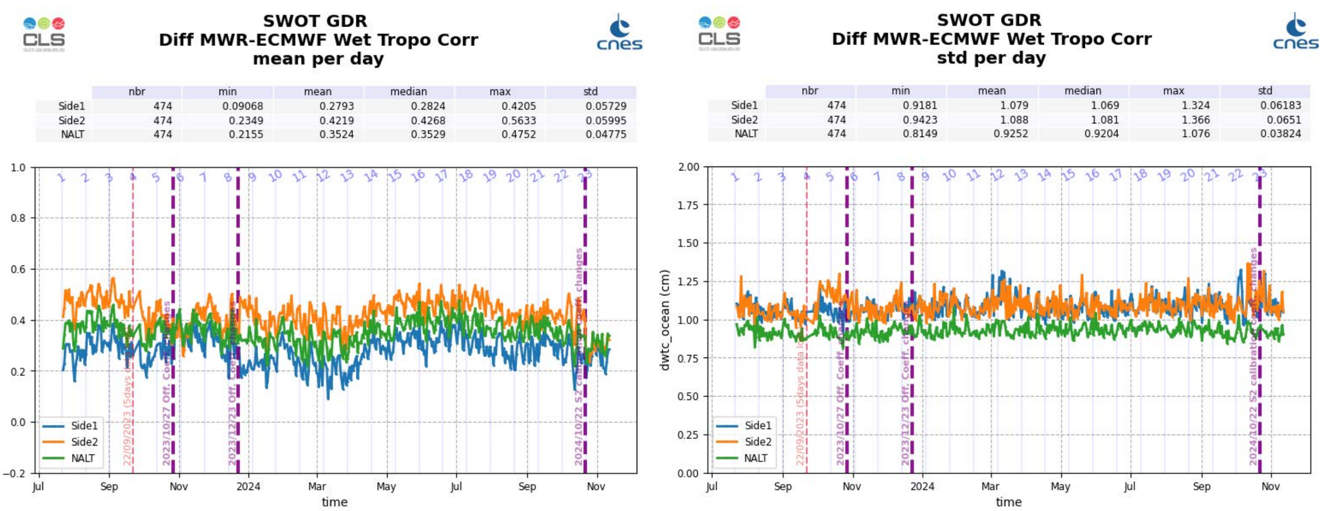

Figure 54: Daily monitoring of the mean of the Wet Tropospheric Correction for the AMR S1 (blue), AMR S2 (orange) and Nadir (green) from Cycle 1 to Cycle 23

The other radiometer products (Water Vapor Content, Cloud Liquid Water Content, Atmospheric Attenuation for the Sigma 0) are interpolated the same way as WTC and can be compared to values issued from the ECMWF model too, as shown in figure 55, assessing the good temporal stability of the Atmospheric Attenuation.

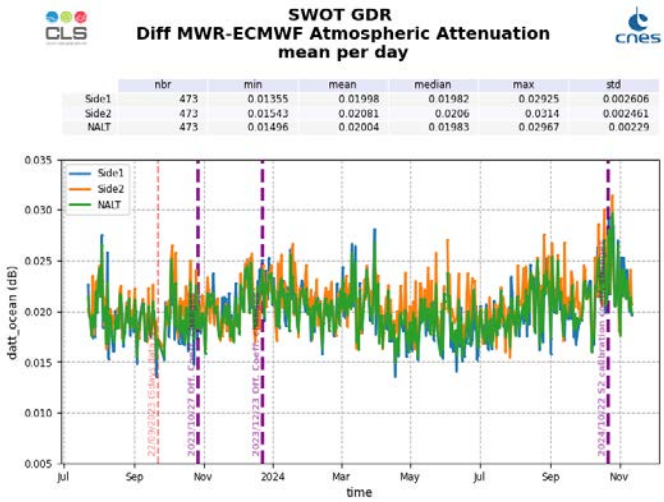

Figure 55: Daily monitoring of the mean of the Wet Tropospheric Correction for the AMR S1 (blue), AMR S2 (orange) and Nadir (green) from Cycle 1 to Cycle 23

5.2. Intercalibration monitoring

To assess the intercalibration between the two sides of the radiometer, the gradient between each Side 1 AMR measurements and the closer Side 2 AMR measurements is calculated for the three brightnesses temperatures and the Wet Tropospheric Correction. This monitoring allows to detect any instrumental drift affecting one of the SWOT radiometer beams, which whould increase the gradient between the two beams. In addition, excessive differences in measurements between the two beams would affect the quality of the interpolation at Nadir. Figure 56 shows the brightnesses temperatures gradients between the two radiometers. The difference is smaller and stable for the 23.4 GHz (which is the main contributor of the Wet Tropospheric Correction) than for the other two. However, after the 22/10/2024 calibration, the S1/S2 gradient is greatly reduced for the three channels, fluctuating around 0.3 Kelvin.

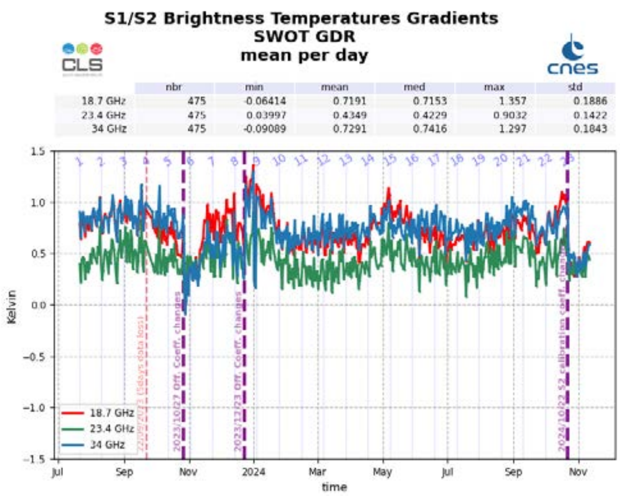

Figure 56: Daily monitoring of the mean S1/S2 gradients of brightness temperatures, for the 18.7 Ghz channel (blue), the 23.4 GHz channel (green) and the 34 GHz channel (red) from Cycle 1 to Cycle 23

Figure 57 shows the Wet Tropospheric Correction gradient between the two radiometers and between the radiometers and the nadir. This difference is stable overall, at around 1 mm, and becomes near null after the change in radiometers calibration coefficients on 22/10/2024

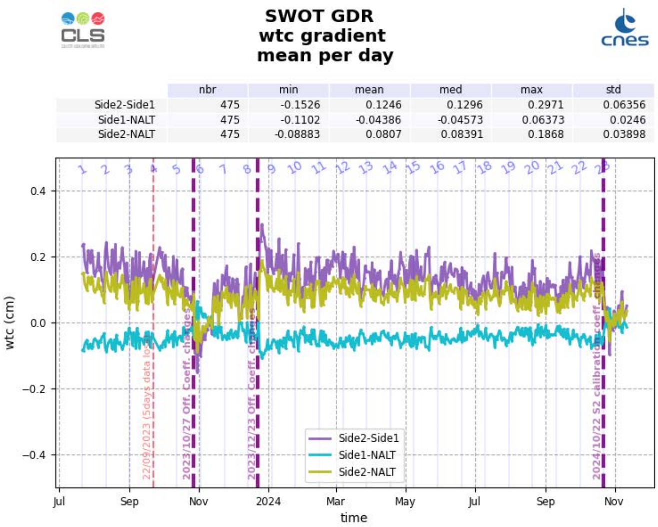

Figure 57: Daily monitoring of the wet tropospheric correction gradient between AMR Side 1 and AMR Side 2 (purple), AMR Side 1 and Nadir (cyan)

5.3. Global Performance of the Wet Tropospheric Correction

The main quality criterion of the WTC from the radiometers is the difference in variance at 10 days at the crossover points between a SSH (sea surface height) calculated with radiometer WTC and a SSH calculated with the model WTC. As the variance of the SSH is supposed to be very low at 10 days, the variance is assumed to be mainly due to correction (WTC or other). Thus, if the use of the radiometer WTC instead of model WTC reduces the SSH variance at crossover, it indicates that the radiometer improves the WTC estimation compared to the model.
Figure 58 shows the difference of variance between the SSH with radiometer WTC (interpolated at nadir) and the SSH with model WTC for SWOT Nadir with a year and a half of data, with a selection to avoid areas with high oceanic variability, shallow waters and high latitudes. The Nadir interpolated WTC reduces the variance of about -1.5 cm² on average, which indicates a good performance of the WTC interpolated on the nadir track.

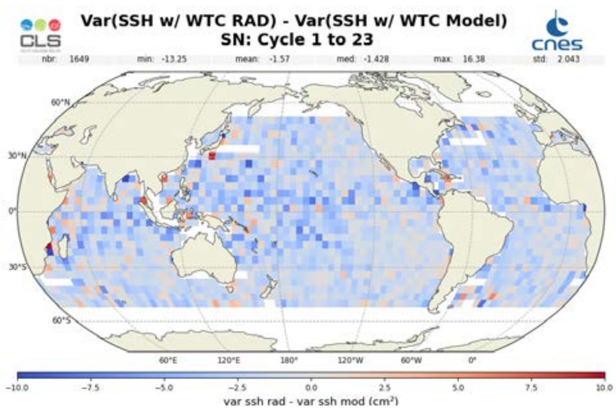

Figure 58: Difference of variance between the SSH with Nadir interpolated WTC and the SSH with model with geographical selection, from cycle 1 to cycle 23

5.4. Impact of the loss of validity of a side on the Nadir interpolation

Some measurements made by the radiometer can be rejected, due to the presence of rain, ice, or land. In some cases, the parts rejected will be so important on one of the sides that the nadir interpolation will use only measurements from the opposite side, creating a discontinuity in the Wet Tropospheric Correction at Nadir, and thus in the Sea Surface Height measurement. However, the interpolation is actually still considered valid by the interpolation quality flag. Figure **??** shows an example where the measures from the AMR S2 are rejected due to the presence of rain cells in its track and are not used in the nadir interpolation. In this area, a bump appears in the WTC interpolated at nadir, which is almost identical to the WTC from the AMR S1, but it still considered as valid.

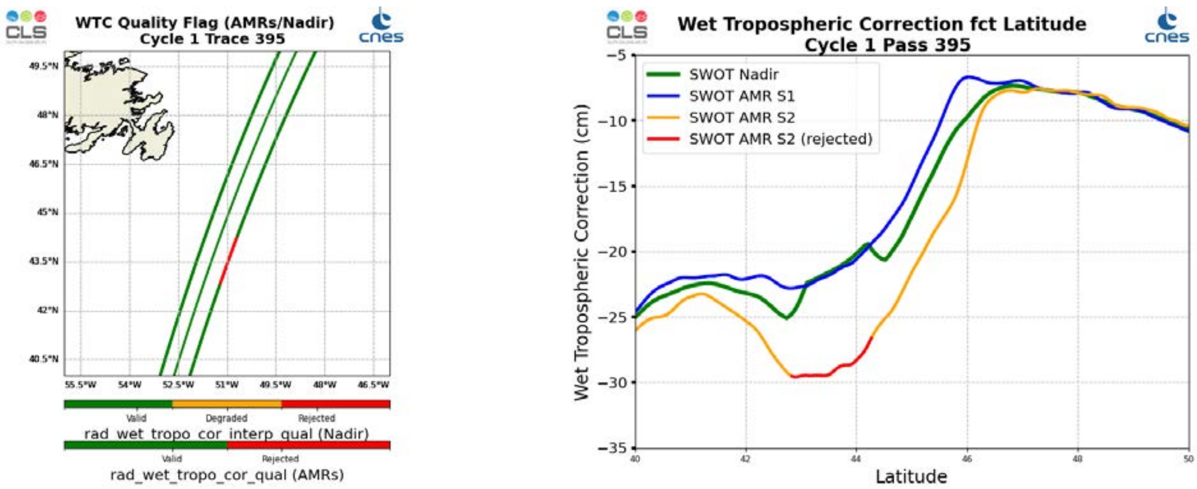

Figure 59: Left: Validity of the Wet Tropospheric Correction for both AMRs and Nadir on Cycle 1 pass 395 (Green: Valid, Orange: Degraded (only for Nadir), red: Rejected). Right: Evolution of the Wet Tropospheric Correction for both AMR sides (S1: blue, S2: orange/red) and Nadir (green) on Cycle 1 Pass 395, on the same area that the left figure

In open ocean, 1.31% of the nadir point in open ocean are affected by this situation (computed on cycle 1 to 5). An update of the interpolation quality flag will be provided in the GDR-S2 reprocessing to considered as "degraded" all these points where the interpolation is made with only one radiometer beam.

6 Assesment from crossover analysis

6.1. Overview

Sea Surface Height crossover differences are the SSH differences between ascending and descending passes where they cross each other. Sea Surface Height is computed as follow:

$$SSH(corrected) = Orbit - AltimeterRange - \sum(GeophysicalCorrections)$$

with for SWOT Nadir:Orbit = CNES orbit for GDR products, and

$$\begin{aligned}
\sum(GeophysicalCorrections) &= Non\ parametric\ sea\ state\ bias\ correction \\
&+ Dual\ frequency\ ionospheric\ correction\ (filtered) \\
&+ Radiometer\ wet\ troposphere\ correction \\
&+ Dry\ troposphere\ correction \\
&+ Dynamical\ atmospheric\ correction \\
&+ Ocean\ tide\ correction\ (including\ loading\ tide\ and\ non\ equilibrium\ tide) \\
&+ Internal\ tide\ correction \\
&+ Earth\ tide\ height \\
&+ Pole\ tide\ height
\end{aligned}$$

Sea Surface Height crossover differences are the SSH (corrected) differences between ascending and descending passes where they cross each other. Crossover differences are systematically analysed to estimate data quality. SSH crossover differences are computed from the valid data, with a maximum time lag of 10 days, in order to limit the effects of ocean variability which are a source of error in the performance estimation. The mean SSH crossover differences should ideally be close to zero and standard deviation should ideally be small.

Nevertheless, SSH varies also within 10 days, especially in high variability areas. Furthermore, due to lower data availability (due to seasonal sea ice coverage), models of several geophysical corrections are less precise in high latitude. Therefore, an additional geographical selection - removing shallow waters, areas of high ocean variability and high latitudes (> |50| deg) - is applied.

6.2. Monomission crossovers

The daily mean of SSH differences is plotted in figure 60. Mean of SSH differences at crossovers is almost null showing the stability of measurements for this diagnostic.
After data editing, applying additional geographical selection and SWOT Nadir standards, the crossover standard deviation for the period between cycle 001 and cycle 023 is about 5.03 cm in MLE4.

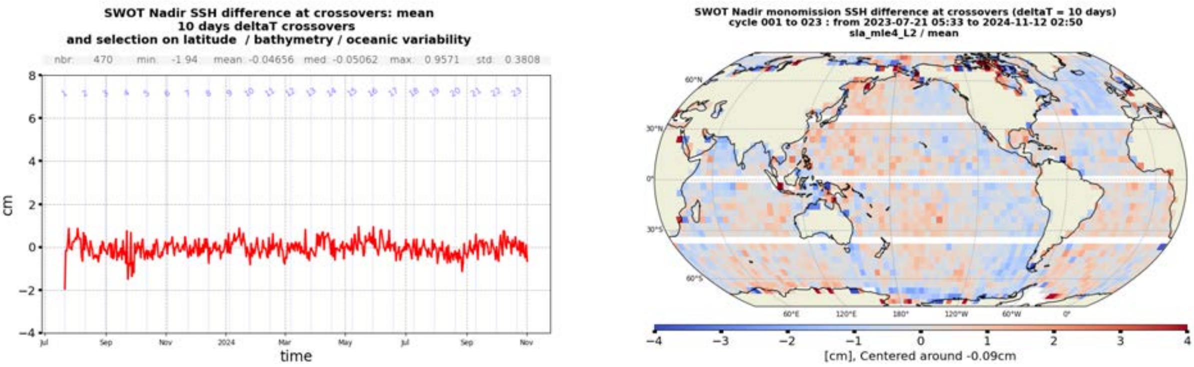

Figure 60: Mean SSH difference at crossovers

The daily standard deviation or variance of SSH crossovers differences are plotted in figure 61 after applying geographical criteria (bathymetry, latitude, oceanic variability).
This metric allows to estimate the system noise by dividing by $\sqrt{2}$ (which leads to 3.56 cm).

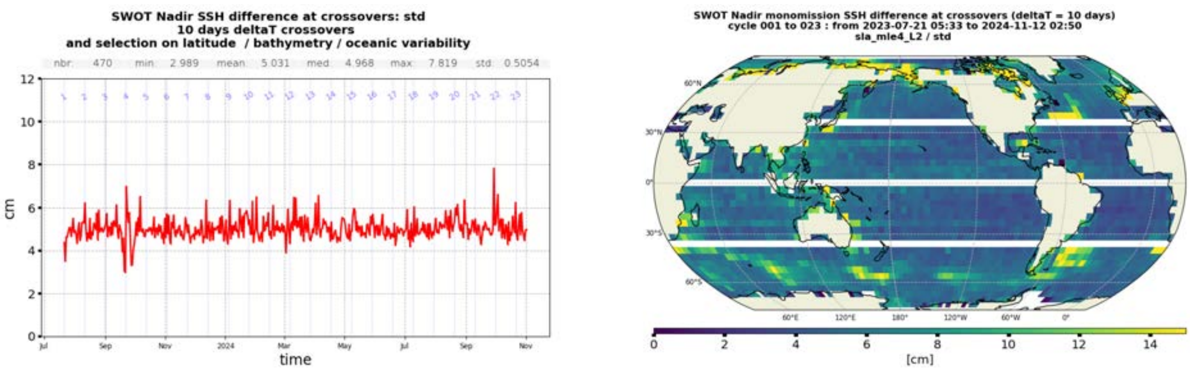

Figure 61: Std SSH difference at crossovers

6.3. Multimission crossovers

Dual-mission crossover performances are computed between SWOT Nadir GDR-F and Sentinel-6A-MF GDR-F and presented figure 62. Mean SLA differences at SWOT Nadir/Sentinel-6A-MF crossovers is quite stable and around 1.015 cm in average. Figure 63 shows seasonal differences.

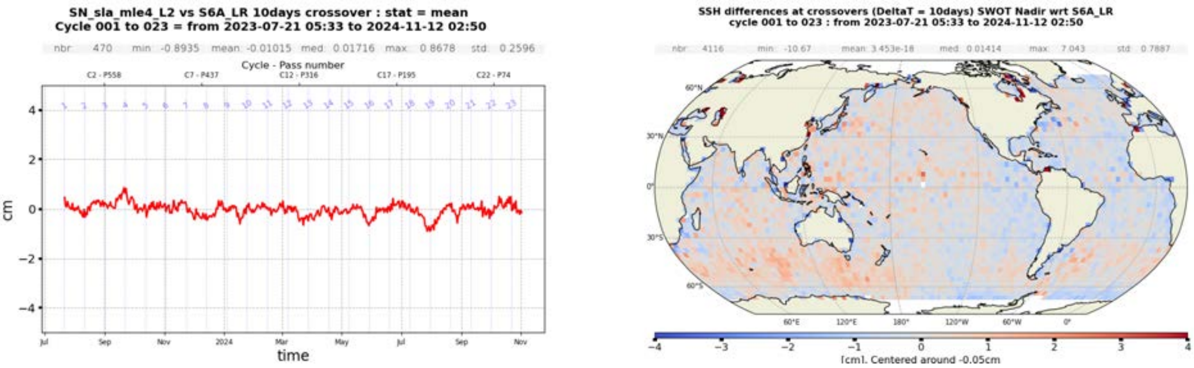

Figure 62: Mean SSH difference at crossovers between SWOT Nadir MLE4 and Sentinel-6 MF LR MLE4

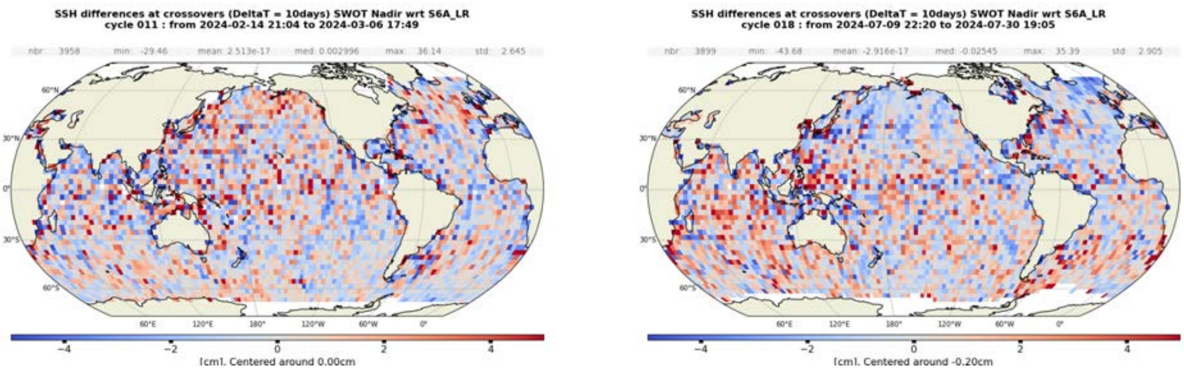

Figure 63: Mean SSH difference at crossovers between SWOT Nadir MLE4 and Sentinel-6 MF LR MLE4 for a winter cycle (left) and a summer cycle (right)

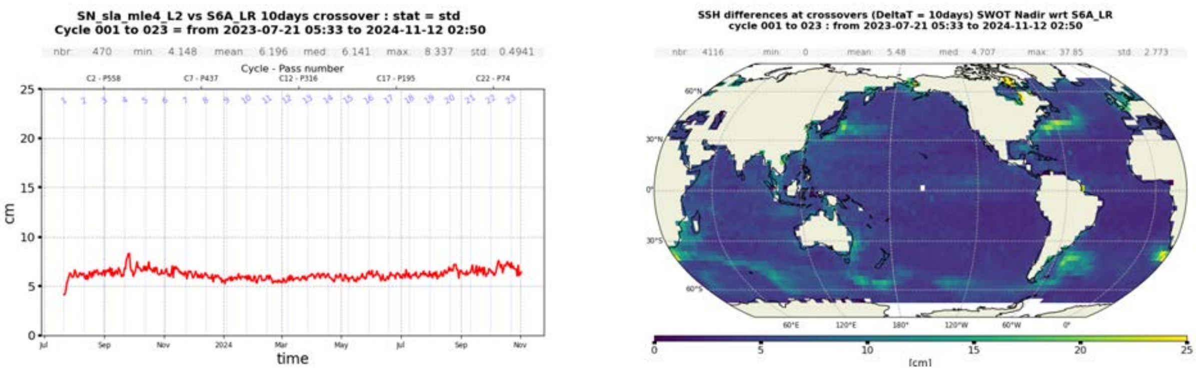

Figure 64: STD Daily monitoring of SSH difference at crossovers between SWOT Nadir MLE4 and Sentinel-6 MF LR MLE4

7 SLA along-track analysis

The Sea Surface Height Anomaly (or SLA) is the most well-known parameter estimated from altimetry. It corresponds to the elevation of sea surface, with respect to a reference called Mean Sea Surface (Mean Sea Surface (MSS)), generated by oceanic variability and climatic phenomena (such as Gulf stream current, El Nino, ...).
It is computed as follow:

$$SLA = Orbit - AltimeterRange - \sum(GeophysicalCorrections) - MSS$$

The details of the geophysical corrrections for SWOT Nadir can be found in previous section 6.1..
SLA analysis is a complementary indicator to estimate the altimetry system performances. It allows to study the evolution of SLA mean (detection of jump, abnormal trend or geographical correlated biases), and also the evolution of the SLA variance highlighting the long-term stability of the altimetry system performances.

The daily monitoring of mean SLA for SWOT Nadir is computed on figure 65.

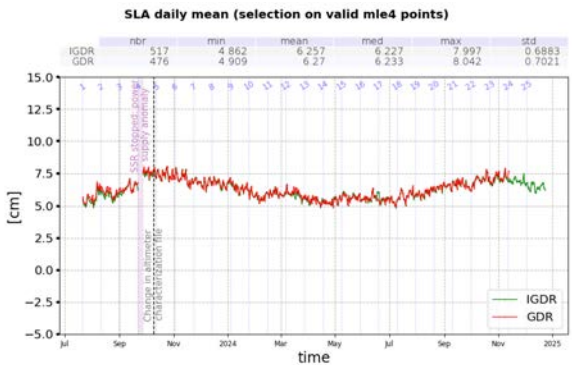

Figure 65: Cyclic monitoring of along-track mean SLA

The monitoring of SLA standard deviation has been computed for the SWOT Nadir mission (figure 66). Note that this metric is very dependant to the MSS reference solution used to compute SLA.
SWOT Nadir shows an good stability in terms of SLA standard deviation.

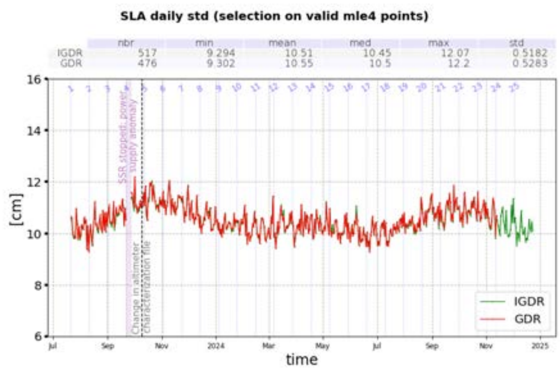

Figure 66: Daily monitoring of along-track SLA standard deviation.

8 Conclusions

SWOT Nadir was launched on December 16th, 2022. Since July 07th, 2023, SWOT Nadir was on its operational 21-days orbit phase.
The main points of the performance assessment are summarized below:

- Ocean data availability is excellent with a percentage of 97.4% including ground station anomaly.
- Data quality is also very good with 2.76% of rejected measurements over ocean (after removing sea ice data).
- The altimeter parameters analysis highlights a quite stable behaviour over the period.
- At crossovers, SWOT Nadir shows good performances with a standard deviation of 5.03cm and a good consistency with the Sentinel-6A-MF reference mission.

Known issue: The current interpolation of radiometer data on the nadir track currently requires the two AMR sides to be defined and valid. When one AMR side is invalid (quality_flag_rad_wet_tropo_cor_qual), the nadir WTC can be affected by interpolation artifacts. Users who want to remove this subset of measurements can check the validity of the radiometer data and flags in the Radiometer L2 product (L2 RAD). In the next release, the SWOT Nadir processing will be updated to natively handle this border case: the radiometer flag (rad_wet_tropo_cor_interp_qual) in the L2 NALT will inform end-users of this degraded radiometer interpolation. In a future release, we plan to revisit the radiometer interpolation algorithm to mitigate or remove interpolation artifacts altogether.

Known issue: Users should also keep in mind that estimated wind speed has a 80cm bias with respect to the model until wind calibration is performed.

9 References

References

[1] Courcol B. Sentinel-6A validation and cross calibration activities (Annual report 2022) at https://www.aviso.altimetry.fr/fileadmin/documents/calval/validation_report/S6A/SALP-RP-MA-EA-23618-CLS_Sentinel6A_AnnualReport_2022_v1_2.pdf

[2] Jason-3 Wet Path Delay Correction provided by https://doi.org/10.5067/J3L2G-PDCOR

[3] Analysis of the Sentinel-6A SLA biais correction at https://www.aviso.altimetry.fr/fileadmin/documents/data/tools/bias_S6ASAR_L2PL3_forORR.pdf

[4] Jason-3 product handbook available at https://www.aviso.altimetry.fr/fileadmin/documents/data/tools/hdbk_j3.pdf

[5] Jason-3 GDR-F standard : ready for operational switch at https://meetings.aviso.altimetry.fr/fileadmin/user_upload/tx_ausyclsseminar/files/CVL_J3_GDRF_ready_v02_ostst2020_02.pdf

[6] SWOT Science Data Products User Handbook available at https://www.earthdata.nasa.gov/s3fs-public/2024-06/D-109532_SWOT_UserHandbook_20240502.pdf

[7] Flamant B. Jason-3 validation and cross calibration activities (Annual report 2022). https://www.aviso.altimetry.fr/fileadmin/documents/calval/validation_report/J3/AnnualReport_J3_2022.pdf

[8] Flamant B. Jason-3 validation and cross calibration activities (Annual report 2021). https://www.aviso.altimetry.fr/fileadmin/documents/calval/validation_report/J3/SALP-RP-MA-EA-23528-CLS_Jason3_AnnualReport_2021_v1-3.pdf

[9] Roinard H. Jason-3 validation and cross calibration activities (Annual report 2020). https://www.aviso.altimetry.fr/fileadmin/documents/calval/validation_report/J3/SALP-RP-MA-EA-23473-CLS_Jason-3_AnnualReport2020_v1-1.pdf

[10] Roinard H. Jason-3 validation and cross calibration activities (Annual report 2019). https://www.aviso.altimetry.fr/fileadmin/documents/calval/validation_report/J3/SALP-RP-MA-EA-23399-CLS_Jason-3_AnnualReport2019_v1-1.pdf

[11] Roinard H. Jason-3 validation and cross calibration activities (Annual report 2017). https://www.aviso.altimetry.fr/fileadmin/documents/calval/validation_report/J3/SALP-RP-MA-EA-23187-CLS_Jason-3_AnnualReport2017_v1-2.pdf

[12] Roinard H. Jason-2 validation and cross calibration activities (Annual report 2017). https://www.aviso.altimetry.fr/fileadmin/documents/calval/validation_report/J2/annual_report_j2_2017.pdf

[13] Nencioli Francesco, Roinard Hélène, Bignalet-Cazalet Francois. 2021. Filtering ionospheric correction from altimetry dual-frequencies solution. DOI 10.24400/527896/a02- 2021.001. Available at https://www.aviso.altimetry.fr/fileadmin/documents/data/tools/NT-Nencioli_FilteredIonosphericCorrection.pdf

[14] Jason-3 validation of GDR-F data over ocean https://www.aviso.altimetry.fr/fileadmin/documents/calval/validation_report/J3/SALP-RP-MA-EA-23480-CLS_Jason3_Reprocessing_Report_v1-2.pdf

[15] Brown G.S., “The average impulse response of a rough surface and its application”, *IEEE Transactions on Antenna and Propagation*, Vol. AP 25, N1, pp. 67-74, Jan. 1977.

[16] Thibaut, P. O.Z. Zanifé, J.P. Dumont, J. Dorandeu, N. Picot, and P. Vincent, 2002. Data editing: The MQE criterion. *Paper presented at the Jason-1 and TOPEX/Poseidon Science Working Team Meeting, New-Orleans (USA), 21-23 October*.

[17] Obligis, E., L. Eymard, M. Ablain, B. Picard, J.F. Legeais, Y. Faugere and N. Picot, 2010. The wet tropospheric correction for altimetry missions: A mean sea level issue.*Oral presentation at OSTST meeting, Lisbon, Portugal*. Available at http://www.aviso.oceanobs.com/fileadmin/documents/OSTST/2010/oral/19_Tuesday/OBLIGIS.pdf.

[18] Updates available for DUACS products. https://www.aviso.altimetry.fr/en/data/product-information/updates-and-reprocessing/ssalto/duacs-product-changes-and-updates.html

[19] Mean Sea Level informations in AVISO. https://www.aviso.altimetry.fr/en/data/products/ocean-indicators-products/mean-sea-level.html

[20] A. Guerou. SALP annual report (2021) of Mean Sea Level Activities. Reference: SALP-RP-MA-EA-23541-CLS

[21] R. Samant, M. Prange 2023. Climate-driven 21st century Caspian Sea level decline estimated from CMIP6 projections https://www.nature.com/articles/s43247-023-01017-8

[22] Bocquet M. and Fleury S. and Piras F. and Rinne E. and Sallila H. and Garnier F. and Rémy F. 2023. Arctic sea ice radar freeboard retrieval from the European Remote-Sensing Satellite (ERS-2) using altimetry: toward sea ice thickness observation from 1995 to 2021. https://tc.copernicus.org/articles/17/3013/2023/

[23] Guérin A., Piras F., Cuvillon N., Homerin A., Le Gac S., Maraldi C., Bignalet-Cazalet F., Alves M., and Rey L. 2024. Description and In-Flight Assessment of the POSEIDON-3C Altimeter of the SWOT Mission. *Remote Sensing*, **16**(22), 4183. https://www.mdpi.com/2072-4292/16/22/4183.